



The trilinear Higgs self-couplings at $\mathcal{O}(\alpha_t^2)$ in the CP-violating NMSSM

Christoph Borschensky^{1,a}, Thi Nhung Dao^{2,b}, Martin Gabelmann^{3,c}, Margarete Mühlleitner^{1,d}, Heidi Rzehak^{4,e}

¹ Institute for Theoretical Physics, Karlsruhe Institute of Technology, Wolfgang-Gaede-Str. 1, 76131 Karlsruhe, Germany

² Faculty of Fundamental Sciences, Phenikaa University, Hanoi 12116, Vietnam

³ Deutsches Elektronen-Synchrotron DESY, Notkestr. 85, 22607 Hamburg, Germany

⁴ Institute for Theoretical Physics, University of Tübingen, Auf der Morgenstelle 14, 72076 Tübingen, Germany

Received: 12 October 2022 / Accepted: 8 January 2023
© The Author(s) 2023

Abstract In supersymmetric theories the Higgs boson masses are derived quantities where higher-order corrections have to be included in order to match the measured Higgs mass value at the precision of current experiments. Closely related through the Higgs potential are the Higgs self-interactions. In addition, the measurement of the trilinear Higgs self-coupling provides the first step towards the reconstruction of the Higgs potential and the experimental verification of the Higgs mechanism *sui generis*. In this paper, we advance our prediction of the trilinear Higgs self-couplings in the CP-violating Next-to-Minimal Supersymmetric extension of the SM (NMSSM). We provide the $\mathcal{O}(\alpha_t^2)$ corrections in the gaugeless limit at vanishing external momenta. The higher-order corrections turn out to be larger than the corresponding mass corrections but show the expected perturbative convergence. The inclusion of the loop-corrected effective trilinear Higgs self-coupling in gluon fusion into Higgs pairs and the estimate of the theoretical uncertainty due to missing higher-order corrections indicate that the missing electroweak higher-order corrections may be significant.

Contents

1	Introduction
2	The tree-level NMSSM
2.1	The Higgs boson sector
2.2	The top/stop sector

3	The loop-corrected couplings
3.1	Definition
3.2	One- and two-loop corrections
4	Set-up of the calculation and of the numerical analysis
4.1	Tools, checks and NMSSMCALC release
4.2	The parameter scan
5	Investigation of specific benchmark points
5.1	Impact on the effective trilinear Higgs self-coupling
5.2	Impact on the Higgs-to-Higgs decays
6	Scatter plots
6.1	The trilinear Higgs self-coupling
6.2	Correlation between trilinear Higgs self-coupling and mass
7	Higgs pair production
8	Conclusions
	References

1 Introduction

The measurement of the trilinear Higgs self-coupling is one of the most important tasks at the LHC and future colliders [1]. It is the first step towards the experimental reconstruction of the Higgs potential and hence the direct experimental verification of the Higgs mechanism *sui generis* [2–4]. In the Standard Model (SM), it is accessible through the challenging measurement of Higgs pair production at colliders. In models with extended Higgs sectors, the Higgs self-couplings are also involved in Higgs-to-Higgs decays. Through the Higgs potential, the trilinear Higgs self-coupling is related to the Higgs boson mass. While in the SM the Higgs mass is an ad hoc input parameter, in supersymmetric theories [5–18] it is derived from the parameters of the model. In

^a e-mail: christoph.borschensky@kit.edu

^b e-mail: nhung.daothi@phenikaa-uni.edu.vn (corresponding author)

^c e-mail: martin.gabelmann@desy.de

^d e-mail: margarete.muehlleitner@kit.edu

^e e-mail: heidi.rzehak@itp.uni-tuebingen.de

the Minimal Supersymmetric extension of the SM (MSSM) [19–22] the Higgs quartic couplings are given in terms of the gauge couplings leading to an upper bound of the tree-level mass of the order of the Z boson mass so that considerable higher-order corrections are required to shift the SM-like Higgs boson mass to the observed value of 125.09 GeV [23]. In the Next-to-MSSM (NMSSM) [24–35] the situation is somewhat more relaxed due to the tree-level contribution stemming from the inclusion of the additional complex singlet field. In the last years, a lot of effort has been put to provide precise predictions for the Higgs mass values at higher loop level both in the MSSM and the NMSSM. For recent reviews, see [36,37]. For the trilinear Higgs self-couplings the corresponding corrections have not yet been provided at the same level of precision as for the masses. In the MSSM, the one-loop corrections to the effective trilinear couplings have been provided many years ago in [38–40]. The process-dependent corrections to heavy scalar MSSM Higgs decays into a lighter Higgs pair have been calculated in [41,42]. The two-loop $\mathcal{O}(\alpha_t\alpha_s)$ SUSY-QCD corrections to the top/stop-loop induced corrections have been made available within the effective potential approach in [43]. In the NMSSM, we provided the full one-loop corrections for the CP-conserving NMSSM [44]. They are sizeable so that the inclusion of the two-loop corrections is mandatory to reduce the theoretical uncertainties due to missing higher-order corrections. Consequently, we subsequently calculated the two-loop $\mathcal{O}(\alpha_t\alpha_s)$ corrections in the limit of vanishing external momenta in [45], in the CP-violating NMSSM. The full one-loop corrections to the Higgs-to-Higgs decays and other on-shell two-body decays were implemented in [46]. For corrections to the trilinear Higgs self-couplings in non-supersymmetric (non-SUSY) Higgs models, see for example Refs. [47–52] for one-loop and Refs. [53–56] for two-loop results, and Refs. [57–66] for the process-dependent Higgs-to-Higgs decays at one-loop level.

In this paper we continue our effort in increasing the precision for the predictions of the trilinear Higgs self-couplings in the context of the NMSSM. We calculate the two-loop corrections at $\mathcal{O}(\alpha_t^2)$ to the trilinear Higgs self-couplings of the complex NMSSM. They are obtained in the limit of zero external momenta and vanishing gauge couplings. We consistently apply the same renormalisation schemes as in our computation of the loop-corrections to the Higgs boson masses, based on a mixed on-shell- $\overline{\text{DR}}$ renormalisation in the Higgs sector and the possibility to choose between on-shell (OS) and $\overline{\text{DR}}$ renormalisation in the top/stop sector. Our corrections have been implemented in our Fortran code NMSSMCALC [67,68] and can be downloaded from the URL: <https://www.itp.kit.edu/~maggie/NMSSMCALC/>

The paper is organized as follows. In Sect. 2 we introduce the tree-level sectors of the NMSSM that are relevant for our calculation and set up our notation. In Sect. 3 we give

the definitions for the loop-corrected effective trilinear Higgs self-couplings and for the loop corrections to the Higgs-to-Higgs decays. We specify the approximations that we apply and the renormalisation schemes that we use. In Sect. 4 we briefly present the set-up of our numerical analysis and the scan that we performed. Sections 5 to 7 are dedicated to our numerical analysis. In Sect. 5 we discuss the impact of our corrections on the effective trilinear Higgs self-couplings and on the Higgs-to-Higgs decays for two specific parameter points, in Sect. 6 we investigate these effects for our whole sample to get a more general picture. The effects of our corrections in the context of Higgs pair production are analysed in Sect. 7. Our conclusions are given in Sect. 8.

2 The tree-level NMSSM

In order to set our notation we briefly introduce the two sectors relevant for the renormalisation, the Higgs and the top/stop sectors. While the computation of the $\mathcal{O}(\alpha_t^2)$ contributions to the Higgs self-energies and tadpoles involves neutralinos and charginos, they do not need to be renormalised as vertices and propagators with these particles only enter at the two-loop level. For the definition of the electroweakino masses and mixing angles in the gaugeless limit we refer to Ref. [69]. We work in the \mathbb{Z}_3 symmetric NMSSM including CP violation. For the computation of the two-loop corrections to the trilinear Higgs self-couplings of the neutral Higgs bosons at $\mathcal{O}(\alpha_t\alpha_s + \alpha_t^2)$ we apply the gaugeless limit and follow the notation of our previous calculations [45,69–71]. Note that in contrast to the MSSM, the trilinear and quartic Higgs couplings in the NMSSM do not vanish in the gaugeless limit, but involve the parameters $\lambda, \kappa, A_\lambda, A_\kappa$. The NMSSM superpotential is given by

$$\begin{aligned} \mathcal{W}_{\text{NMSSM}} = & \left[y_e \hat{H}_d \cdot \hat{L} \hat{E}^c + y_d \hat{H}_d \cdot \hat{Q} \hat{D}^c - y_u \hat{H}_u \cdot \hat{Q} \hat{U}^c \right] \\ & - \lambda \hat{S} \hat{H}_d \cdot \hat{H}_u + \frac{1}{3} \kappa \hat{S}^3, \end{aligned} \quad (1)$$

in terms of the quark and lepton superfields $\hat{Q}, \hat{U}, \hat{D}, \hat{L}, \hat{E}$, the Higgs doublet superfields \hat{H}_d, \hat{H}_u and the singlet superfield \hat{S} . Charge conjugated fields are denoted by the superscript c . We have suppressed color and generation indices for better readability. The symplectic product $x \cdot y = \epsilon_{ij} x^i y^j$ ($i, j = 1, 2$) is built with the anti-symmetric tensor $\epsilon_{12} = \epsilon^{12} = 1$. Working in the CP-violating NMSSM, the parameters λ, κ are in general complex. All y_x ($x = e, d, u$) are taken to be real by rephasing the left- and right-handed Weyl-spinor fields as $x_{L,R} \rightarrow x_{L,R} e^{i\varphi_{L,R}}$. In our computation, the Yukawa couplings y_x are assumed to be diagonal in flavour space, and we only include y_t while all other Yukawa couplings are set

to zero. The soft SUSY breaking Lagrangian is given by

$$\begin{aligned} \mathcal{L}_{\text{soft, NMSSM}} = & -m_{H_d}^2 H_d^\dagger H_d - m_{H_u}^2 H_u^\dagger H_u - m_{\tilde{Q}}^2 \tilde{Q}^\dagger \tilde{Q} \\ & - m_{\tilde{L}}^2 \tilde{L}^\dagger \tilde{L} - m_{\tilde{u}_R}^2 \tilde{u}_R^* \tilde{u}_R - m_{\tilde{d}_R}^2 \tilde{d}_R^* \tilde{d}_R \\ & - m_{\tilde{e}_R}^2 \tilde{e}_R^* \tilde{e}_R - ([y_e A_e H_d \cdot \tilde{L} \tilde{e}_R^* \\ & + y_d A_d H_d \cdot \tilde{Q} \tilde{d}_R^* - y_u A_u H_u \cdot \tilde{Q} \tilde{u}_R^*] + \text{h.c.}) \\ & - \frac{1}{2} (M_1 \tilde{B} \tilde{B} + M_2 \tilde{W}_i \tilde{W}_i + M_3 \tilde{G} \tilde{G} + \text{h.c.}) \\ & - m_S^2 |S|^2 + \left(\lambda A_\lambda S H_d \cdot H_u - \frac{1}{3} \kappa A_\kappa S^3 + \text{h.c.} \right), \end{aligned} \quad (2)$$

where again quark and lepton generation indices are suppressed. The \tilde{Q} , \tilde{u}_R , \tilde{d}_R and \tilde{L} , \tilde{e}_R denote the complex scalar components of the corresponding quark and lepton superfields. The soft SUSY breaking gaugino mass parameters M_i ($i = 1, 2, 3$) of the bino, wino and gluino fields \tilde{B} , \tilde{W}_i ($i = 1, 2, 3$) and \tilde{G} as well as the soft SUSY breaking trilinear couplings A_x ($x = \lambda, \kappa, u, d, e$) are complex in the CP-violating NMSSM in contrast to the soft SUSY breaking mass parameters of the scalar fields, m_X^2 ($X = S, H_d, H_u, \tilde{Q}, \tilde{u}_R, \tilde{d}_R, \tilde{L}, \tilde{e}_R$), which are real.

2.1 The Higgs boson sector

The tree-level Higgs boson potential is obtained from $\mathcal{L}_{\text{soft, NMSSM}}$, the F -terms of $\mathcal{W}_{\text{NMSSM}}$ and the D -terms originating from the gauge sector,

$$\begin{aligned} V_H = & (|\lambda S|^2 + m_{H_d}^2) H_d^\dagger H_d + (|\lambda S|^2 + m_{H_u}^2) H_u^\dagger H_u + m_S^2 |S|^2 \\ & + \frac{1}{8} (g_2^2 + g_1^2) (H_d^\dagger H_d - H_u^\dagger H_u)^2 + \frac{1}{2} g_2^2 |H_d^\dagger H_u|^2 \\ & + |\kappa S^2 - \lambda H_d \cdot H_u|^2 + \left[\frac{1}{3} \kappa A_\kappa S^3 - \lambda A_\lambda S H_d \cdot H_u + \text{h.c.} \right]. \end{aligned} \quad (3)$$

In the gaugeless limit, the $U(1)_Y$ and $SU(2)_L$ gauge couplings $g_1 \rightarrow 0$ and $g_2 \rightarrow 0$ while $\tan \theta_W = g_2/g_1$ is kept constant, with θ_W being the weak mixing angle. This is equivalent to the limit of vanishing electric charge and tree-level vector boson masses, $e, M_W, M_Z \rightarrow 0$, while keeping $\tan \theta_W$ constant.

The Higgs boson fields are expanded around their vacuum expectation values (VEVs) v_u, v_d , and v_s as

$$\begin{aligned} H_d = & \begin{pmatrix} \frac{v_d + h_d + i a_d}{\sqrt{2}} \\ h_d \end{pmatrix}, \quad H_u = e^{i\varphi_u} \begin{pmatrix} h_u^+ \\ \frac{v_u + h_u + i a_u}{\sqrt{2}} \end{pmatrix}, \\ S = & \frac{e^{i\varphi_s}}{\sqrt{2}} (v_s + h_s + i a_s), \end{aligned} \quad (4)$$

where $\varphi_{u,s}$ denote the CP-violating phases. We can replace the three VEVs by $\tan \beta$, the SM VEV v and the effective μ

parameter μ_{eff} as

$$t_\beta \equiv \tan \beta = v_u/v_d \quad (5)$$

$$v^2 = v_u^2 + v_d^2 \approx (246 \text{ GeV})^2 \quad (6)$$

$$\mu_{\text{eff}} = \frac{e^{i\varphi_s}}{\sqrt{2}} v_s \lambda. \quad (7)$$

Note that the MSSM limit is smoothly retraced by taking the limit $\lambda, \kappa \rightarrow 0, v_s \rightarrow \infty$ and at the same time keeping μ_{eff} and κ/λ constant. From the Higgs potential of Eq. (3) we obtain the tree-level tadpoles, the Higgs mass matrices and the trilinear Higgs self-couplings. For the tadpole coefficients we have

$$(t)_l = t_{\phi_l} = \left. \frac{\partial V_H}{\partial \phi_l} \right|_{\phi=0}, \quad l = 1, \dots, 6, \quad (8)$$

with

$$\phi = (h_d, h_u, h_s, a_d, a_u, a_s)^T. \quad (9)$$

Only five of the tadpoles are independent, since $t_{a_u} = t_{a_d}/t_\beta$. The neutral Higgs mass matrix in the interaction basis is obtained as

$$\mathcal{M}_{\phi_l \phi_m} = \left. \frac{\partial^2 V_H}{\partial \phi_l \partial \phi_m} \right|_{\phi=0} \quad (10)$$

and the charged one as ($r, s = 1, 2$)

$$\mathcal{M}_{h_r^+ h_s^-} = \left. \frac{\partial V_H}{\partial h_r^{c,\dagger} \partial h_s^c} \right|_{h^c=0}, \quad \text{with } h^c = (h_d^-, h_u^+). \quad (11)$$

The trilinear couplings which need to be renormalised at two-loop level for the calculation of the $\mathcal{O}(\alpha^2)$ corrections in this paper, are obtained as

$$\lambda_{\phi_l \phi_m \phi_n} \equiv \lambda_{lmn} = \left. \frac{\partial^3 V_H}{\partial \phi_l \partial \phi_m \partial \phi_n} \right|_{\phi=0}. \quad (12)$$

The explicit expressions for the tadpoles and the squared mass matrices $\mathcal{M}_{\phi\phi}$ and $\mathcal{M}_{h^+h^-}$ are given in Ref. [69] and those for the trilinear Higgs self-couplings can be found in the Appendix of Ref. [45]. The neutral Higgs mass eigenstates are obtained by a two-fold rotation that first separates the Goldstone component through the rotation $\mathcal{R}^G(\beta_n)$, *i.e.* it transforms from the basis $(h_d, h_u, h_s, a_d, a_u, a_s)$ to $(h_d, h_u, h_s, a, a_s, G^0)$, and afterwards rotates into the mass basis $(h_1, h_2, h_3, h_4, h_5, G^0)$ with the rotation matrix \mathcal{R} ,

$$\mathcal{M}_{hh} = \mathcal{R}^G(\beta_n) \mathcal{M}_{\phi\phi} (\mathcal{R}^G(\beta_n))^T \quad (13)$$

$$\begin{aligned} \mathcal{M}'_{hh} = & \mathcal{R} \mathcal{M}_{hh} \mathcal{R}^T \\ = & \text{diag} \left(m_{h_1}^2, m_{h_2}^2, m_{h_3}^2, m_{h_4}^2, m_{h_5}^2, m_{G^0}^2 \right), \end{aligned} \quad (14)$$

where the neutral Goldstone boson mass is equal to the Z boson mass, $m_{G^0} = M_Z$, in 't Hooft Feynman gauge. It vanishes in the gaugeless limit. The charged Higgs fields

are rotated to the mass eigenstates with a single rotation $\mathcal{R}^{G^-}(\beta_c)$,

$$\mathcal{R}^{G^-}(\beta_c)\mathcal{M}_{h+h^-}(\mathcal{R}^{G^-}(\beta_c))^T = \text{diag}(m_{G^\pm}^2, M_{H^\pm}^2). \quad (15)$$

In the 't Hooft Feynman gauge the charged Goldstone boson mass is equal to the charged W boson mass, $m_{G^\pm} = M_W$, and vanishes in the gaugeless limit. At tree-level the rotation angles β_n and β_c coincide with β , $\beta_c = \beta_n = \beta$. They are distinguished here as β_n and β_c are mixing angles and do not need to obtain a counterterm which is not the case for β that arises from the ratio of the VEVs. It has to be renormalised and receives a non-vanishing counterterm. After the renormalisation they are set equal to the tree-level value of β again. Our tree-level masses are denoted by small letters m , apart from the charged Higgs boson mass. When we talk about loop-corrected masses, they are denoted by capital M . In our renormalisation of the trilinear coupling we will adopt the same renormalisation conditions as those used in the two-loop corrections of the masses.

We apply the SUSY Les Houches Accord (SLHA) [72, 73] and in accordance with this accord decompose the complex parameters A_λ and A_κ into their imaginary and real parts. While in our program code NMSSMCALC also λ and κ are read in in terms of their real and complex part in accordance with the SLHA, internally, we choose a different, more convenient, parametrisation. We decompose λ and κ into their absolute values and phases φ_λ and φ_κ . We note that the phases enter the tree-level Higgs mass matrix in two combinations together with φ_u and φ_s ,

$$\varphi_y = \varphi_\kappa - \varphi_\lambda + 2\varphi_s - \varphi_u \quad (16)$$

$$\varphi_w = \varphi_\kappa + 3\varphi_s, \quad (17)$$

where φ_y is the only CP-violating phase at tree level in the Higgs sector. If $\varphi_y = 0$, the CP-even components, h_u, h_d, h_s , hence do not mix with the CP-odd ones, a_d, a_u, a_s . We use the tadpole conditions to replace $\text{Im}A_{\lambda,\kappa}$ as well as $m_{H_{u,d,S}}^2$ by the tadpole parameters t_{a_d,a_s} and $t_{h_{d,u,s}}$, respectively, cf. Ref. [69] for details.

In NMSSMCALC, we have two possibilities to choose the set of input parameters in the Higgs sector, either

$$\left\{ t_{h_d}, t_{h_u}, t_{h_s}, t_{a_d}, t_{a_s}, M_{H^\pm}^2, v, s_{\theta_W}, e, \tan \beta, |\lambda|, v_s, |\kappa|, \text{Re}A_\kappa, \varphi_\lambda, \varphi_\kappa, \varphi_u, \varphi_s \right\}, \quad (18)$$

or

$$\left\{ t_{h_d}, t_{h_u}, t_{h_s}, t_{a_d}, t_{a_s}, v, s_{\theta_W}, e, \tan \beta, |\lambda|, v_s, |\kappa|, \text{Re}A_\lambda, \text{Re}A_\kappa, \varphi_\lambda, \varphi_\kappa, \varphi_u, \varphi_s \right\}. \quad (19)$$

In the first choice the charged Higgs mass is an input parameter while in the second one we have $\text{Re}A_\lambda$ as an input parameter.

2.2 The top/stop sector

For the calculation of the Higgs self-couplings at the order $\mathcal{O}(\alpha_t^2)$, the top/stop sector needs to be renormalised at $\mathcal{O}(\alpha_t)$. The top mass and the top-quark Yukawa coupling are related as,

$$m_t = \frac{v_u y_t}{\sqrt{2}} e^{i(\varphi_u + \varphi_L - \varphi_R)}, \quad (20)$$

with m_t and y_t being real in our convention. Applying the freedom of choice of the phases φ_L, φ_R of the left- and right-handed top-quark fields, we define $\varphi_L = -\varphi_R = -\varphi_u/2$. Thereby the stop mass matrix in the $(\tilde{t}_L, \tilde{t}_R)^T$ basis in the gaugeless limit is given by

$$\mathcal{M}_{\tilde{t}} = \begin{pmatrix} m_{\tilde{Q}_3}^2 + m_t^2 & m_t \left(A_t^* e^{-i\varphi_u} - \frac{\mu_{\text{eff}}}{\tan \beta} \right) \\ m_t \left(A_t e^{i\varphi_u} - \frac{\mu_{\text{eff}}^*}{\tan \beta} \right) & m_{\tilde{t}_R}^2 + m_t^2 \end{pmatrix} \quad (21)$$

$$\text{diag}(m_{\tilde{t}_1}^2, m_{\tilde{t}_2}^2) = \mathcal{U}^{\tilde{t}} \mathcal{M}_{\tilde{t}} \mathcal{U}^{\tilde{t}\dagger}, \quad (22)$$

where $\mathcal{U}^{\tilde{t}}$ denotes the rotation matrix for the left- and right-handed stop fields $\tilde{t}_{L,R}$ into the mass eigenstates $\tilde{t}_{1,2}$. We set the bottom quark mass to zero everywhere so that the right-handed sbottom states decouple and only left-handed sbottom states appear in the computation. In the stop sector the parameters to be renormalised at one-loop level are

$$m_t, m_{\tilde{Q}_3}, m_{\tilde{t}_R} \text{ and } A_t. \quad (23)$$

3 The loop-corrected couplings

3.1 Definition

The renormalised trilinear Higgs self-coupling $\hat{\lambda}_{ijk}$ at two-loop order between the interaction states h_i, h_j and h_k is given by

$$\hat{\lambda}_{ijk} = \lambda_{ijk} + \Delta^{(1)}\lambda_{ijk} + \Delta^{(2)}\lambda_{ijk}. \quad (24)$$

Here the indices i, j, k refer to the interaction basis $(h_d, h_u, h_s, a_d, a_u, a_s)$. We denote the trilinear tree-level Higgs self-coupling by λ_{ijk} and the one- and two-loop corrections to it by $\Delta^{(1)}\lambda_{ijk}$ and $\Delta^{(2)}\lambda_{ijk}$, respectively. The explicit expressions for the tree-level couplings in the interaction basis are given in Appendix A of [45].

Applying the description in [45], we define the so-called effective trilinear Higgs self-couplings as follows. Both one-

loop and two-loop corrections are computed in the approximation of zero external momenta, more specifically:

- In the one-loop corrections, $\Delta^{(1)}\lambda$ (for simplicity, here and in the following we drop the indices 'ijk' where they are not needed), we include only corrections at $\mathcal{O}(\alpha_t)$.¹ These are coming from the top/stop sector and are hence the dominant ones. They have been discussed in detail in [45].
- For the two-loop corrections, $\Delta^{(2)}\lambda$, we include the dominant contributions of $\mathcal{O}(\alpha_t\alpha_s)$ and $\mathcal{O}(\alpha_t^2)$,

$$\Delta^{(2)}\lambda = \Delta^{\alpha_t\alpha_s}\lambda + \Delta^{\alpha_t^2}\lambda, \tag{25}$$

where the QCD corrections $\Delta^{\alpha_t\alpha_s}\lambda$ have been computed in [45]. In this paper the $\Delta^{\alpha_t^2}\lambda$ corrections are calculated for the first time.

- After calculating $\hat{\lambda}_{ijk}$ in the interaction basis $(h_d, h_u, h_s, a_d, a_u, a_s)$ we rotate it first to the basis $(h_d, h_u, h_s, a, a_s, G^0)$ with the rotation matrix $\mathcal{R}^G(\beta_n)$ to single out the couplings with the neutral Goldstone bosons as

$$\hat{\lambda}_{nmq} = \mathcal{R}_{ni}^G \mathcal{R}_{mj}^G \mathcal{R}_{qk}^G \hat{\lambda}_{ijk}. \tag{26}$$

- To obtain the effective trilinear couplings in the mass eigenstate basis we use the loop-corrected rotation matrix $\mathcal{R}^{l,\text{eff}}$. This matrix diagonalizes the loop-corrected mass matrix evaluated in the approximation of vanishing external momentum,

$$\hat{\lambda}_{abc}^{\text{eff}} = \mathcal{R}_{an}^{l,\text{eff}} \mathcal{R}_{bm}^{l,\text{eff}} \mathcal{R}_{cq}^{l,\text{eff}} \hat{\lambda}_{nmq}, \tag{27}$$

where the indices a, b, c refer to the mass basis $(H_1, H_2, H_3, H_4, H_5)$ and n, m, q to the interaction basis (h_d, h_u, h_s, a, a_s) . The matrix $\mathcal{R}^{l,\text{eff}}$ is a 5×5 matrix and returned as an SLHA output of NMSMCalc in the block NMHMXC. Note that we denote the loop-corrected Higgs boson masses by capital letters (H_i) and the tree-level ones by lower letters (h_i) .

We will later also calculate the Higgs-to-Higgs decays where we have to ensure the proper on-shell conditions of

¹ The full one-loop correction in the zero momentum approximation to the effective trilinear couplings has been computed and analysed in our previous publication [44]. We verified that for the effective coupling of the SM-like Higgs boson the contribution from other sectors at one-loop level is less than 2% for the parameter points chosen in our study. For parameter points that contain very light scalars and large mixing between singlet- and doublet-like states the one-loop contribution from the Higgs sector can be much larger than 2%. However, in such cases the zero momentum approximation used to compute the effective couplings is not reliable anymore.

the external Higgs bosons. In this case the one-loop corrections $\Delta^{(1)}\lambda$ include the full electroweak corrections together with non-vanishing momentum effects. They have been computed by us in the context of the CP-conserving and CP-violating NMSSM in Refs. [44,45], respectively. The two-loop part $\Delta^{(2)}\lambda$ contains the $\mathcal{O}(\alpha_t\alpha_s)$ and $\mathcal{O}(\alpha_t^2)$ part, computed in the zero-momentum approximation as described above. Throughout, at two-loop order we apply the gaugeless limit. In order to ensure the proper on-shell conditions of the Higgs bosons, to the maximum extent possible in the context of our calculation, the amplitude for the decay process $H_a \rightarrow H_b + H_c$ is computed by including the effect from the finite wave-function renormalisation factor matrix \mathbf{Z} which is defined by

$$\mathcal{M}_{H_a \rightarrow H_b + H_c} = \mathcal{R}_{an}^l \mathcal{R}_{bm}^l \mathcal{R}_{cq}^l \hat{\lambda}_{nmq}, \tag{28}$$

where

$$\mathcal{R}^l = \mathbf{Z}\mathcal{R}, \tag{29}$$

with \mathcal{R} being the matrix that rotates the interaction eigenstates $(h_d, h_u, h_s, a, a_s, G^0)$ to the tree-level mass eigenstates $(h_1, h_2, h_3, h_4, h_5, G^0)$. The definition of the matrix \mathbf{Z} can be found in Ref. [44] for the CP-conserving case and Ref. [46] for the CP-violating case.²

3.2 One- and two-loop corrections

To be consistent, we compute the one- and two-loop corrections to the trilinear Higgs self-couplings in accordance with the corresponding one- and two-loop corrections to the Higgs boson masses. This means we use the same renormalisation conditions in the higher-order corrections to the trilinear couplings as the ones we used in our computation for the masses. For our mass calculations, the detailed presentation of the one-loop corrections can be found in [74,75] and of the two-loop corrections up to order $\mathcal{O}(\alpha_t\alpha_s)$ in [70], to order $\mathcal{O}(\alpha_t^2)$ in [69] and to order $\mathcal{O}((\alpha_t + \alpha_\lambda + \alpha_\kappa)^2)$ in [71], together with the corresponding renormalisation conditions and the explicit definitions of the counterterms. The one-loop corrections to the trilinear Higgs self-couplings in the real NMSSM have been presented in [44] and to two-loop order $\mathcal{O}(\alpha_t\alpha_s)$ in the CP-violating NMSSM in [45]. Throughout our computations we apply a mixed on-shell (OS)- $\overline{\text{DR}}$ renormalisation scheme. In the two-loop corrections which require the renormalisation of the top/stop sector we provide the option to choose between OS and $\overline{\text{DR}}$ renormalisation. All details can be found in the respective papers. Here we focus on a minimal description and refer the reader for further information to this literature.

² For the complex MSSM this has been derived in Ref. [41].

In case the charged Higgs mass is used as independent input the parameters related to the Higgs sector that need to be renormalised are given by³

$$\underbrace{t_{h_d}, t_{h_u}, t_{h_s}, t_{a_d}, t_{a_s}, M_{H^\pm}^2, v}_{\text{on-shell scheme}}, \quad (30)$$

$$\underbrace{\tan \beta, |\lambda|, v_s, |\kappa|, \text{Re}A_\kappa, \varphi_\lambda, \varphi_\kappa, \varphi_u, \varphi_s}_{\overline{\text{DR}} \text{ scheme}},$$

and by

$$\underbrace{t_{h_d}, t_{h_u}, t_{h_s}, t_{a_d}, t_{a_s}, v}_{\text{on-shell scheme}}, \quad (31)$$

$$\underbrace{\tan \beta, |\lambda|, v_s, |\kappa|, \text{Re}A_\lambda, \text{Re}A_\kappa, \varphi_\lambda, \varphi_\kappa, \varphi_u, \varphi_s}_{\overline{\text{DR}} \text{ scheme}},$$

for $\text{Re}(A_\lambda)$ as independent input. Note, that we apply the gaugeless limit in which the gauge boson masses, M_Z and M_W , and the electric coupling e vanish, but the VEV defined as $v = 2M_W s_{\theta_W}/e$ is kept as an on-shell input parameter. Only the ratio of the gauge boson counterterms and their respective masses enter the counterterm of the on-shell defined v ; the corresponding counterterms are calculated in the approximation of vanishing external momenta. At one-loop $\mathcal{O}(\alpha_t)$ and two-loop $\mathcal{O}(\alpha_t \alpha_s)$ the VEV counterterm contributes to the finite part of the effective trilinear couplings but at two-loop $\mathcal{O}(\alpha_t^2)$ the VEV counterterm does not contribute. For the Higgs fields, which need to be renormalised as well, we choose $\overline{\text{DR}}$ conditions. The details of the renormalisation procedure and the counterterms are given in the above mentioned papers so that we do not repeat them here.

The one-loop corrections $\Delta^{(1)}\lambda$ of the trilinear Higgs self-couplings can be decomposed as

$$\Delta^{(1)}\lambda = \Delta^{(1)}\lambda^{\text{UR}} + \Delta^{(1)}\lambda^{\text{CT}}, \quad (32)$$

where the first term denotes the unrenormalised part given by the genuine one-loop diagrams. For the $\mathcal{O}(\alpha_t)$ corrections, they comprise the one-loop diagrams with top and stops running in the loops and we restrict ourselves to the gaugeless limit. For the trilinear couplings used in the Higgs-to-Higgs decays we include the complete one-loop corrections at non-vanishing gauge couplings. The explicit expressions for the order $\mathcal{O}(\alpha_t)$ corrections to the trilinear self-couplings are given in App. B and the counterterm expressions $\Delta^{(1)}\lambda^{\text{CT}}$ are given in App. C of Ref. [45].

The two-loop corrections $\Delta^{(2)}\lambda$ of the trilinear Higgs self-couplings are composed of

$$\Delta^{(2)}\lambda = \Delta^{(2)}\lambda^{\text{UR}} + \Delta^{(2)}\lambda^{\text{CT1L}} + \Delta^{(2)}\lambda^{\text{CT2L}}. \quad (33)$$

The unrenormalised part $\Delta^{(2)}\lambda^{\text{UR}}$ consists of the genuine two-loop diagrams contributing at order $\mathcal{O}(\alpha_t \alpha_s)$ and $\mathcal{O}(\alpha_t^2)$. Some sample diagrams for the newly computed $\mathcal{O}(\alpha_t^2)$ are depicted in Fig. 1. In the approximation of zero external momenta all two-loop three-point functions can be written in terms of products of one-loop integrals or the two-loop tadpole integral. Their analytic expressions are given in the literature [76–82]. The counterterm contributions $\Delta^{(2)}\lambda^{\text{CT1L}}$ arise from one-loop diagrams containing top and stop contributions combined with one insertion of a counterterm of the order $\mathcal{O}(\alpha_s)$ (for the $\mathcal{O}(\alpha_t \alpha_s)$ corrections) or the order $\mathcal{O}(\alpha_t)$ (for the $\mathcal{O}(\alpha_t^2)$ corrections) from the top/stop sector. The counterterm contribution $\Delta^{(2)}\lambda^{\text{CT2L}}$ consists of the $\mathcal{O}(\alpha_t \alpha_s)$ and $\mathcal{O}(\alpha_t^2)$ counterterms and is manifestly zero when only top/stop contributions are considered.

4 Set-up of the calculation and of the numerical analysis

4.1 Tools, checks and NMSSMCALC release

For the computation of the loop-corrected trilinear Higgs self-couplings we made use of our setup for our computation of the loop-corrected Higgs masses [71]. There we used SARAH 4.14.3 [83–88] to generate the FeynArts model file including the vertex counterterms. The file was then used in FeynArts 3.10 [89,90] to generate all required one- and two-loop Feynman diagrams for the calculation of the corrections to the trilinear Higgs self-couplings. The evaluation of the fermion traces and the tensor reduction of the one- and two-loop integrals and the amplitudes with the counterterm-inserted diagrams was done with the help of FeynCalc 9.2.0 [91,92] and its TARCER plugin [93]. We performed three independent calculations which all agreed. We also explicitly checked the ultraviolet (UV)-finiteness of the loop-corrected Higgs self-couplings.

The calculation of the trilinear Higgs self-couplings at one- and two-loop order as well as the Higgs-to-Higgs decays including these corrections, has been implemented in NMSSMCALC [67] both for the CP-conserving and the CP-violating NMSSM. The new NMSSMCALC version 5.1 can be downloaded from the URL: <https://www.itp.kit.edu/~maggie/NMSSMCALC/>

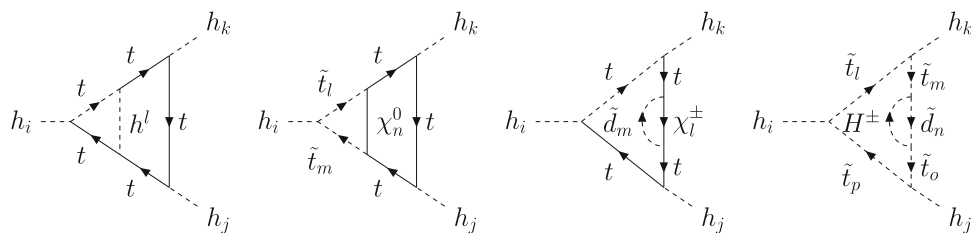
The input file `inp.dat` includes the option to choose between the different loop orders in the trilinear couplings and correspondingly the Higgs-to-Higgs-decay widths. The effective trilinear Higgs self-couplings as defined above are given out in the output file.

4.2 The parameter scan

For the numerical discussion of our results we used the data set that we had generated for Ref. [71] by performing a scan

³ Note, that for the two-loop $\mathcal{O}(\alpha_t^2)$ corrections computed in this publication, we only need to renormalise the parameters of the top/stop sector.

Fig. 1 Sample diagrams contributing to the trilinear Higgs self-coupling at $\mathcal{O}(\alpha_t^2)$



in the NMSSM parameter space and keeping only those data sets that are in accordance with the relevant experimental constraints. We briefly summarise them here for convenience of the reader. We ensured compatibility with experimental constraints from the Higgs data by using `HiggsBounds` 5.9.0 [94–96] and `HiggsSignals` 2.6.1 [97]. The required effective NMSSM Higgs boson couplings normalised to the corresponding SM values were generated with `NMSSMCALC`. For valid points, χ^2 computed by `HiggsSignals-2.6.1` needs to be consistent with an SM χ^2 within 2σ .⁴ For this analysis, we checked the sample again with the updated `HiggsBounds` 5.10.2 and `HiggsSignals` 2.6.2⁵ and found that more than 90% of the points (and in particular the two benchmark points discussed below) are still in the allowed region. We required one of the neutral CP-even Higgs bosons, called h from now on, to behave as the SM-like Higgs boson and to have a mass in the range

$$122 \text{ GeV} \leq m_h \leq 128 \text{ GeV}, \tag{34}$$

when including the two-loop corrections at $\mathcal{O}((\alpha_t + \alpha_\lambda + \alpha_\kappa)^2 + \alpha_t \alpha_s)$ in the default mixed $\overline{\text{DR}}$ -OS scheme specified above and with OS renormalisation in the top/stop and charged Higgs boson sectors as well as an infrared mass regulator M_R with $M_R^2 = 10^{-3} \mu_R^2$ to treat the Goldstone problem.⁶ For details, we refer to [71]. The SM input values have been chosen as [98, 99]

$$\begin{aligned} \alpha(M_Z) &= 1/127.955, & \alpha_s^{\overline{\text{MS}}}(M_Z) &= 0.1181, \\ M_Z &= 91.1876 \text{ GeV}, & M_W &= 80.379 \text{ GeV}, \\ m_t &= 172.74 \text{ GeV}, & m_b^{\overline{\text{MS}}}(m_b^{\overline{\text{MS}}}) &= 4.18 \text{ GeV}, \\ m_c &= 1.274 \text{ GeV}, & m_s &= 95.0 \text{ MeV}, \\ m_u &= 2.2 \text{ MeV}, & m_d &= 4.7 \text{ MeV}, \\ m_\tau &= 1.77682 \text{ GeV}, & m_\mu &= 105.6584 \text{ MeV}, \\ m_e &= 510.9989 \text{ keV}, & G_F &= 1.16637 \cdot 10^{-5} \text{ GeV}^{-2}. \end{aligned} \tag{35}$$

⁴ In `HiggsSignals-2.6.1`, the SM χ^2 obtained with the latest data set is 84.44. We allowed the NMSSM χ^2 to be in the range [78.26, 90.62].

⁵ In `HiggsSignals-2.6.2`, the SM χ^2 obtained with the latest data set is 89.62.

⁶ Note that the Goldstone problem does not occur in the trilinear Higgs self-couplings at the considered loop order $\mathcal{O}(\alpha_t(\alpha_s + \alpha_t))$. It appears at $\mathcal{O}((\alpha_t + \alpha_\lambda + \alpha_\kappa)^2)$ which we use only in the Higgs mass calculation in order to check whether the Higgs mass of the SM-like Higgs boson is in accordance with the experimental result.

Table 1 Scan ranges for the random scan over the NMSSM parameter space, with $\tilde{X} = \tilde{b}_R, \tilde{L}, \tilde{\tau}$ and $i = b, \tau, \kappa$. Values of $\kappa = \lambda \cdot \xi > 0.7$ are omitted

Parameter	Scan range [TeV]
M_{H^\pm}	[0.5, 1]
M_1, M_2	[0.4, 1]
M_3	2
μ_{eff}	[0.1, 1]
$m_{\tilde{Q}_3}, m_{\tilde{\tau}_R}$	[0.4, 3]
$m_{\tilde{X} \neq \tilde{Q}_3, \tilde{\tau}_R}$	3
Parameter	Scan range
$\tan \beta$	[1, 10]
λ	[0.01, 0.7]
κ	$\lambda \cdot \xi$
ξ	[0.1, 1.5]
A_t	[-3, 3] TeV
$A_{i \neq t}$	[-2, 2] TeV

In accordance with the SLHA format the soft SUSY breaking masses and trilinear couplings are understood as $\overline{\text{DR}}$ parameters at the scale

$$\mu_0 = M_{\text{SUSY}} = \sqrt{m_{\tilde{Q}_3} m_{\tilde{\tau}_R}}. \tag{36}$$

This is also the renormalisation scale that we use in the computation of the higher-order corrections. The scan ranges of our input parameters are given in Table 1. Note, that both λ and κ are required to remain below 0.7 in order to roughly ensure perturbativity below the GUT scale. Also $\lambda, \kappa, \mu_{\text{eff}}$ and $\tan \beta$ are understood to be $\overline{\text{DR}}$ parameters at the scale M_{SUSY} according to the SLHA format. For the scan we kept all CP-violating phases equal to zero. We discarded parameter points with any of the following mass configurations,

- (i) $m_{\chi_i^{(\pm)}}, m_{h_i} > 1 \text{ TeV}, m_{\tilde{\tau}_2} > 2 \text{ TeV}$
- (ii) $m_{h_i} - m_{h_j} < 0.1 \text{ GeV}, m_{\chi_i^{(\pm)}} - m_{\chi_j^{(\pm)}} < 0.1 \text{ GeV}$
- (iii) $m_{\chi_1^\pm} < 94 \text{ GeV}, m_{\tilde{\tau}_1} < 1 \text{ TeV}.$

With the first condition (i) we avoid large logarithms in our fixed-order calculation. The second condition (ii) omits degenerate mass configurations for which the two-loop part of the `NMSSMCALC` code is not yet optimised. The third con-

Table 2 P2OS: Mass values in GeV and main components of the neutral Higgs bosons at tree-level, one-loop, two-loop $\mathcal{O}(\alpha_t \alpha_s)$, two-loop $\mathcal{O}(\alpha_t(\alpha_s + \alpha_t))$ and at two-loop $\mathcal{O}(\alpha_{\lambda\kappa}^2)$ obtained by using OS ($\overline{\text{DR}}$) renormalisation in the top/stop sector. Italic numbers relate to states that are dominantly h_u -like. Bold numbers relate to dominantly h_s -like states

	$h_1 [h_u]$	$h_2 [h_s]$	$h_3 [h_d]$	$a_1 [a_s]$	$a_2 [a_d]$
Tree-level	96.86	112.10	926.25	511.34	925.86
One-loop	129.01	<i>135.09</i>	926.69	512.55	925.08
$\mathcal{O}(\alpha_t \alpha_s)$	<i>(116.3)</i>	(130.1)	<i>(926.33)</i>	<i>(512.66)</i>	<i>(925.18)</i>
Two-loop $\mathcal{O}(\alpha_t \alpha_s)$	<i>121.36</i>	129.7	926.37	512.62	925.11
	<i>(121.65)</i>	(130.39)	<i>(926.46)</i>	<i>(512.61)</i>	<i>(925.15)</i>
Two-loop $\mathcal{O}(\alpha_t(\alpha_s + \alpha_t))$	<i>126.09</i>	130.04	926.49	512.62	925.11
	<i>(121.54)</i>	(130.38)	<i>(926.45)</i>	<i>(512.61)</i>	<i>(925.15)</i>
Two-loop $\mathcal{O}(\alpha_{\lambda\kappa}^2)$	<i>125.25</i>	129.91	926.62	511.91	925.07
	<i>(121.67)</i>	(130.20)	<i>(926.52)</i>	<i>(512.12)</i>	<i>(925.14)</i>

dition (iii) takes into account lower limits on the lightest chargino and the lightest stop mass. The experimental limits given by the LHC experiments ATLAS and CMS rely on assumptions of the mass spectra and are often based on simplified models. The quotation of a lower limit therefore necessarily requires a scenario that matches the assumptions made by the experiments. For our parameter scan we therefore chose a conservative approach to apply limits that roughly comply with the recent limits given by ATLAS and CMS [100, 101].

5 Investigation of specific benchmark points

In the following, we present results for two benchmark points. One point is the benchmark point P2OS from our investigation of the Higgs mass corrections at $\mathcal{O}(\alpha_{\lambda\kappa}^2) \equiv \mathcal{O}((\alpha_t + \alpha_\lambda + \alpha_\kappa)^2 + \alpha_t \alpha_s)$ in [71]. The other point is the benchmark point BP10 of Ref. [102]. They have been chosen such that the SM-like Higgs boson mass complies with our required mass window Eq. (34) at $\mathcal{O}(\alpha_{\lambda\kappa}^2)$ when we choose OS renormalisation in the top/stop sector. The charged Higgs mass here and in all other results presented in the following is renormalised OS. The first parameter point P2OS features a large singlet admixture to the h_u -like mass and is defined by the following input parameters:

Parameter Point P2OS: All complex phases are set to zero and the remaining input parameters are given by

$$\begin{aligned}
 |\lambda| &= 0.59, \quad |\kappa| = 0.23, \quad \text{Re}(A_\kappa) = -546 \text{ GeV}, \\
 |\mu_{\text{eff}}| &= 397 \text{ GeV}, \quad \tan \beta = 2.05, \\
 M_{H^\pm} &= 922 \text{ GeV}, \quad m_{\tilde{Q}_3} = 1.2 \text{ TeV}, \\
 m_{\tilde{t}_R} &= 1.37 \text{ TeV}, \quad m_{\tilde{X} \neq \tilde{Q}_3, \tilde{t}_R} = 3 \text{ TeV}, \\
 A_t &= -911 \text{ GeV}, \quad A_{i \neq t, \kappa} = 0 \text{ GeV}, \\
 |M_1| &= 656 \text{ GeV}, \quad |M_2| = 679 \text{ GeV}, \quad M_3 = 2 \text{ TeV}.
 \end{aligned}
 \tag{37}$$

We apply the SLHA format in which μ_{eff} is taken as input parameter. From this we compute v_s by using Eq. (7) (φ_s is set to zero).

Since the trilinear Higgs self-couplings and the mass values are closely related through the Higgs potential a discussion of the higher-order corrections to the trilinear Higgs self-couplings should be completed by the information on the Higgs mass corrections. In Table 2 we hence give the mass values obtained for P2OS at tree level, at one-loop order and at two-loop level at $\mathcal{O}(\alpha_t \alpha_s)$, $\mathcal{O}(\alpha_t(\alpha_s + \alpha_t))$ and the latest computed two-loop order $\mathcal{O}(\alpha_{\lambda\kappa}^2)$ for OS renormalisation in the top/stop sector, and in round brackets those for $\overline{\text{DR}}$ renormalisation in the top/stop sector. Note that the numbers slightly changed compared to those given in [71] due to a bug in the VEV counterterm. The changes are in the sub percentage level.

In the table we also list in square brackets the main singlet/doublet and scalar/pseudoscalar component of each mass eigenstate. At $\mathcal{O}(\alpha_{\lambda\kappa}^2)$ the lightest Higgs boson h_1 obtains a mass of around 125.3 GeV. Since it is h_u -like it couples maximally to top quarks so that the LHC Higgs signal strengths are reproduced and it hence behaves SM-like. In the following plots we will always label the Higgs bosons according to their dominant admixture,⁷ as this determines the Higgs coupling strengths and consequently the size of the loop corrections. This allows us to consistently compare and interpret the impact of the loop corrections.

The second parameter point BP10 features a resonantly enhanced Higgs pair production cross section in gluon fusion and is given by:

Parameter Point BP10: All complex phases are set to zero and the remaining input parameters are given by

$$\begin{aligned}
 |\lambda| &= 0.65, \quad |\kappa| = 0.65, \quad \text{Re}(A_\kappa) = -432 \text{ GeV}, \\
 |\mu_{\text{eff}}| &= 225 \text{ GeV}, \quad \tan \beta = 2.6, \\
 M_{H^\pm} &= 611 \text{ GeV}, \quad m_{\tilde{Q}_3} = 1304 \text{ GeV}, \quad m_{\tilde{t}_R} = 1576 \text{ GeV},
 \end{aligned}$$

⁷ They are mass eigenstates, however. The labeling only refers to the nature of these mass eigenstates.

Table 3 BP10: Mass values in GeV and main components of the neutral Higgs bosons at tree-level, one-loop, two-loop $\mathcal{O}(\alpha_t \alpha_s)$, two-loop $\mathcal{O}(\alpha_t(\alpha_s + \alpha_t))$ and at two-loop $\mathcal{O}(\alpha_{\lambda\kappa}^2)$ obtained by using OS ($\overline{\text{DR}}$) renormalisation in the top/stop sector

	$h_1 [h_u]$	$h_2 [h_s]$	$h_3 [h_d]$	$a_1 [a_s]$	$a_2 [a_d]$
Tree-level	97.21	307.80	626.13	556.71	617.22
One-loop	131.46	299.65	625.96	543.58	615.82
$\mathcal{O}(\alpha_t \alpha_s)$	(114.81)	(299.28)	(625.52)	(543.69)	(616.01)
Two-loop $\mathcal{O}(\alpha_t \alpha_s)$	118.90	299.40	625.78	543.73	615.90
	(120.36)	(299.38)	(625.58)	(543.60)	(615.96)
Two-loop $\mathcal{O}(\alpha_t(\alpha_s + \alpha_t))$	123.53	299.44	625.89	543.73	615.90
	(120.14)	(299.38)	(625.57)	(543.60)	(615.96)
Two-loop $\mathcal{O}(\alpha_{\lambda\kappa}^2)$	122.36	300.27	625.94	543.34	615.91
	(119.97)	(299.90)	(625.65)	(543.47)	(616.01)

$$\begin{aligned}
 m_{\tilde{\chi} \neq \tilde{Q}_3, \tilde{t}_R} &= 3 \text{ TeV}, \\
 A_t &= 46 \text{ GeV}, \quad A_b = -1790 \text{ GeV}, \\
 A_\tau &= -93 \text{ GeV}, \quad A_c = 267 \text{ GeV}, \\
 A_s &= -618 \text{ GeV}, \quad A_\mu = 1851 \text{ GeV}, \\
 A_u &= -59 \text{ GeV}, \quad A_d = -175 \text{ GeV}, \\
 A_e &= 1600 \text{ GeV}, \quad |M_1| = 810 \text{ GeV}, \quad |M_2| = 642 \text{ GeV}, \\
 M_3 &= 2 \text{ TeV}.
 \end{aligned}
 \tag{38}$$

The mass values that are obtained at the different loop levels are summarised in Table 3 for OS ($\overline{\text{DR}}$) renormalisation in the top/stop sector.

The impact of the loop corrections on the Higgs boson masses has been discussed extensively in [71]. Let us therefore here state only the main features. The h_u -like tree-level Higgs mass value changes considerably when one-loop corrections are included, with a smaller change in the $\overline{\text{DR}}$ scheme, as in this scheme we already partly resum higher-order corrections.⁸ The relative $\mathcal{O}(\alpha_t \alpha_s)$ corrections compared to the one-loop result are at the several per-cent level and move the obtained mass values in the two renormalisation schemes closer to each other, whereas the additional inclusion of the $\mathcal{O}(\alpha_t^2)$ corrections increases the difference again (in the OS scheme). The newest corrections at $\mathcal{O}(\alpha_{\lambda\kappa}^2)$ move the two values a little bit closer again.

5.1 Impact on the effective trilinear Higgs self-coupling

In Fig. 2 (left) we present for the parameter point P2OS with the large singlet admixture the effective trilinear Higgs self-coupling $\hat{\lambda}_{111}^{\text{eff}}$, as defined in Eq. (27), of the dominantly h_u -like Higgs boson for OS (full) and $\overline{\text{DR}}$ (dashed) renormalisation in the top/stop sector as a function of the stop

trilinear coupling A_t . The dominantly h_u -like Higgs boson here always is the lightest mass eigenstate. Note, that here and in the following the A_t is always the $\overline{\text{DR}}$ value.⁹ Shown are the results at one-loop order (black), two-loop $\mathcal{O}(\alpha_t \alpha_s)$ (blue) and at the newly calculated two-loop $\mathcal{O}(\alpha_t(\alpha_s + \alpha_t))$ (red). Note that the loop-corrected rotation matrix $\mathcal{R}^{l,\text{eff}}$ for the rotation to the mass eigenstates is taken consistently at the respective loop order. We plot here only the variation of A_t between -500 and $+500$ GeV. In this region the phenomenology at $\mathcal{O}(\alpha_t(\alpha_s + \alpha_t))$ is in accordance with the LHC Higgs data.¹⁰

The steep decrease of the full red curve towards negative A_t values is due to the approach to the cross-over point where the singlet-like and doublet h_u -like Higgs state interchange their roles with respect to their mass ordering. This point is located outside of the shown region in the plot, at $A_t = -900$ GeV, cf. Fig. 3 in Ref. [71]. The interchange of the roles of the two lightest mass eigenstates takes place due to the large singlet admixture for this parameter point which induces the transition between the h_s - and h_u -like interaction state. For the trilinear coupling $\hat{\lambda}_{ijk}$ in the interaction basis after singling out the Goldstone boson, cf. Eq. (26), this of course does not occur. The multiplication with the mixing matrices $\mathcal{R}^{l,\text{eff}}$ causes the mixing of the singlet and doublet states and also mixes in higher orders, as we do not evaluate the mixing matrix multiplication strictly at the considered loop order.

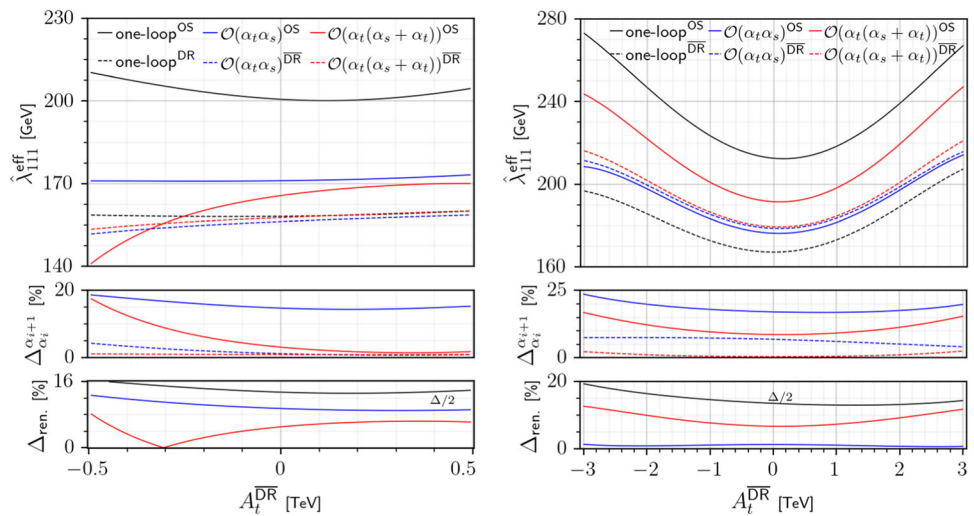
In order to quantify the impact of the new additional corrections we define – for a given renormalisation scheme – the relative change in the trilinear coupling value when going from loop order α_i to the loop order α_{i+1} , which includes the

⁸ In the top/stop sector in accordance with the SLHA approach, which we apply, the top mass is an OS input parameter whereas the soft SUSY breaking mass parameters and trilinear coupling are $\overline{\text{DR}}$ parameters. When we choose the $\overline{\text{DR}}$ renormalisation scheme the top mass has therefore to be converted to the $\overline{\text{DR}}$ scheme. The conversion procedure has been described in Ref. [69], App. C. It includes the renormalisation group running up to the SUSY scale and thereby resums higher orders.

⁹ The corresponding value of A_t^{OS} differs by 0–20% from $A_t^{\overline{\text{DR}}}$ such that the overall shape of the plots remains the same.

¹⁰ Different higher-order corrections to the SM-like Higgs boson mass obviously imply different mass values and mixing angles and hence affect the compatibility with the Higgs data.

Fig. 2 Upper: Effective trilinear coupling $\hat{\lambda}_{111}^{\text{eff}}$ of the h_u -dominated Higgs mass eigenstate as a function of $A_t^{\overline{\text{DR}}}$ for P2OS (left) and BP10 (right) at one-loop order (black), two-loop $\mathcal{O}(\alpha_t\alpha_s)$ (blue) and two-loop $\mathcal{O}(\alpha_t(\alpha_s + \alpha_t))$ (red) in the OS (full) and DR scheme (dashed). Middle: The relative correction as defined in Eq. (39). Lower: The relative renormalisation scheme dependence as defined in Eq. (40) for all three loop orders. The label $\Delta/2$ refers to the black line



next level of λ corrections, as

$$\Delta_{\alpha_i}^{\alpha_{i+1}} = \frac{|\lambda^{\alpha_{i+1}} - \lambda^{\alpha_i}|}{\lambda^{\alpha_i}}. \tag{39}$$

The relative corrections amount to $\Delta_{\text{one-loop}}^{\alpha_t\alpha_s} = 14\text{--}19\%$ in the OS scheme when we include the $\mathcal{O}(\alpha_t\alpha_s)$ corrections beyond one-loop order. When we include the $\mathcal{O}(\alpha_t(\alpha_s + \alpha_t))$ corrections in addition to the available two-loop $\mathcal{O}(\alpha_t\alpha_s)$ corrections the relative change is smaller with $\Delta_{\alpha_t\alpha_s}^{\alpha_t(\alpha_s + \alpha_t)} = 1.5\text{--}18\%$. As expected the relative change decreases with increasing higher-order in the corrections. Note, that the relative corrections can be positive or negative. In the $\overline{\text{DR}}$ scheme the corrections are much smaller. We have for the relative $\mathcal{O}(\alpha_t\alpha_s)$ corrections compared to one-loop order $0.8\text{--}4\%$, and the new corrections change the coupling by about 1%. The reason is that the $\overline{\text{DR}}$ scheme already partly resums higher-order corrections.

The lower panel in Fig. 2 shows the relative change in the corrections to the trilinear Higgs self-coupling at fixed loop order when we change the renormalisation scheme in the top/stop sector,¹¹

$$\Delta_{\text{ren}} = \frac{|\lambda^{m_t(\overline{\text{DR}})} - \lambda^{m_t(\text{OS})}|}{\lambda^{m_t(\overline{\text{DR}})}}. \tag{40}$$

The comparison of the results in the two different renormalisation schemes can be used to estimate the uncertainty on the trilinear Higgs self-coupling due to missing higher-order corrections. As expected, the renormalisation scheme dependence is reduced when more higher-order corrections are included. The renormalisation scheme dependence continuously decreases from one-loop order with $26\text{--}33\%$, to $9\text{--}13\%$ at $\mathcal{O}(\alpha_t\alpha_s)$ and to $0.01\text{--}8\%$ at $\mathcal{O}(\alpha_t(\alpha_s + \alpha_t))$ —the

value of 0.01 at $\mathcal{O}(\alpha_t(\alpha_s + \alpha_t))$ is accidentally small due to the cross-over behaviour.

In Fig. 2 (right) we show our results for the benchmark point BP10. For this point, the relative corrections in the OS scheme are slightly larger than for P2OS. We have $\Delta_{\text{one-loop}}^{\alpha_t\alpha_s} = 17\text{--}24\%$ and $\Delta_{\alpha_t\alpha_s}^{\alpha_t(\alpha_s + \alpha_t)} = 9\text{--}17\%$. In the $\overline{\text{DR}}$ scheme the corrections are smaller, the relative $\mathcal{O}(\alpha_t\alpha_s)$ corrections compared to one-loop order are of $4\text{--}7\%$, and the new corrections change the coupling by $0.4\text{--}2\%$. The renormalisation scheme dependence decreases from one-loop order with $26\text{--}39\%$ to $0.7\text{--}1.4\%$ at $\mathcal{O}(\alpha_t\alpha_s)$. The scheme dependence increases again at $\mathcal{O}(\alpha_t(\alpha_s + \alpha_t))$ where it is $7\text{--}13\%$. This is a behaviour that we already observed in the loop corrections to the Higgs boson masses [69].¹²

In summary, for both benchmark points the inclusion of the new two-loop corrections has an impact of a few per cent and we find a renormalisation scheme dependence of typical two-loop order. The behaviour is similar to the one we found for the Higgs mass corrections.

CP violation In Fig. 3 we show for the parameter point P2OS the loop corrections to the effective trilinear Higgs self-coupling $\hat{\lambda}_{111}^{\text{eff}}$ of the dominantly h_u -like Higgs boson as a function of the CP-violating phase φ_{A_t} of $A_t^{\overline{\text{DR}}}$. The colour and line codes are the same as in Fig. 2. In order to avoid too large singlet-doublet mixing effects we chose $|A_t^{\overline{\text{DR}}}| = 250$ GeV. CP violation due to the phase φ_{A_t} is a loop-induced effect. Since A_t enters at one-loop level, the trilinear Higgs self-coupling shows a dependence on the CP-violating phase, which for this parameter point turns out to be larger in the OS than in the $\overline{\text{DR}}$ renormalisation scheme. The almost flat dependence on the CP-violating phase of the

¹² Incomplete two-loop corrections cannot necessarily be expected to reduce the uncertainty when including further corrections as there might be missing cancellations. The complete two-loop corrected results, however, should reduce the renormalisation scheme dependence compared to the complete one-loop result in a perturbative expansion in the coupling constants.

¹¹ In the $\overline{\text{DR}}$ scheme of the top/stop sector, we have to consistently convert the OS top mass to DR top mass while in the OS scheme all DR inputs, $m_{\overline{Q}_3}^{\overline{\text{DR}}}, m_{\overline{t}_R}^{\overline{\text{DR}}}, A_t^{\overline{\text{DR}}}$, are converted to the $m_{\overline{Q}_3}^{\text{OS}}, m_{\overline{t}_R}^{\text{OS}}, A_t^{\text{OS}}$ values.

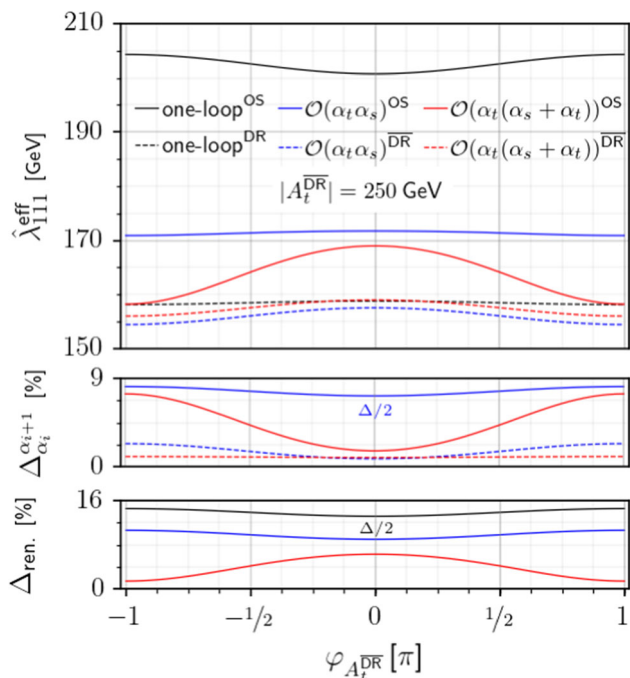


Fig. 3 Effective Higgs self-coupling $\hat{\lambda}_{111}^{\text{eff}}$ of the h_u -dominated Higgs mass eigenstate for P2OS as a function of φ_{A_t} , for $|A_t^{\text{DR}}| = 250$ GeV. Color and line codes are the same as in Fig. 2

OS curve at $\mathcal{O}(\alpha_t \alpha_s)$ is due to accidental cancellations which we explicitly checked. At $\mathcal{O}(\alpha_t(\alpha_s + \alpha_t))$, we see a stronger dependence again. In the $\overline{\text{DR}}$ scheme both two-loop orders show about the same dependence on the phase φ_{A_t} . Note that the measurements of the electric dipole moment (EDM) put severe constraints on the amount of allowed CP violation. The electron imposes the strongest constraints [103], with the current best experimental limit given by the ACME collaboration [104]. After taking into account these constraints, the effect of the CP-violating phases on masses and mixing angles is only marginal and would not affect the overall distribution of the allowed points from a parameter scan of the model.

5.2 Impact on the Higgs-to-Higgs decays

We now turn to the impact of the computed higher-order corrections on the partial decay widths for Higgs-to-Higgs decays. The decay width for the Higgs decay h_i into a Higgs pair $h_j h_k$ is given by

$$\Gamma(h_i \rightarrow h_j h_k) = \frac{\beta^{1/2}(M_{h_i}^2, M_{h_j}^2, M_{h_k}^2)}{16\pi(1 + \delta_{jk})M_{h_i}^3} |\mathcal{M}_{h_i \rightarrow h_j h_k}|^2, \tag{41}$$

where $\beta(x, y, z) = (x - y - z)^2 - 4yz$ is the two-body phase space function and the decay amplitude $\mathcal{M}_{h_i \rightarrow h_j h_k}$ is calculated according to Eq. (28). We show in Fig. 4 (left) the

partial decay width of the doublet-like CP-even Higgs boson h_d into a pair of a SM-like Higgs boson h_u and a singlet-dominated Higgs h_s , $\Gamma(h_d \rightarrow h_u h_s)$, at one-loop level and at two-loop $\mathcal{O}(\alpha_t \alpha_s)$ and $\mathcal{O}(\alpha_t(\alpha_s + \alpha_t))$ for P2OS, as a function of A_t .¹³ This decay is the largest of the Higgs-to-Higgs decays for this parameter point. For BP10 the largest one is given by $h_s \rightarrow h_u h_u$ which we show in Fig. 4 (right). This is also the resonant contribution that increases the production process of an $h_u h_u$ Higgs pair which we will discuss later. We include both the \mathbf{Z} matrix of (29) and the Higgs mass values calculated at the corresponding same loop order as the one for which we calculate the higher-order corrections to the trilinear Higgs self-coupling. This of course also implies that the kinematical factor in the decay amplitude changes with the loop order. For both parameter points, we observe a reduction of both the relative correction and the renormalisation scheme dependence when we move from one- to two-loop order with the effect being less pronounced in the $\overline{\text{DR}}$ than in the OS scheme as the former already partly resums higher-order corrections.

For P2OS the relative corrections for the partial decay width in the OS scheme amount to more than 100% when including the $\mathcal{O}(\alpha_t \alpha_s)$ corrections in addition to the one-loop corrections. The reason is the small one-loop decay width. In the $\overline{\text{DR}}$ scheme the relative corrections amount to 10–14%. The relative effect of the new two-loop corrections is much less as expected and reaches $\Delta_{\alpha_t \alpha_s}^{\alpha_t(\alpha_s + \alpha_t)} = 7\text{--}15\%$ (0.4%) in the OS ($\overline{\text{DR}}$) scheme. The renormalisation scheme dependence decreases from $\mathcal{O}(71\text{--}90\%)$ at one-loop level to a maximum of 13% at two-loop $\mathcal{O}(\alpha_t \alpha_s)$ and at most 14% at two-loop $\mathcal{O}(\alpha_t(\alpha_s + \alpha_t))$. For the benchmark point BP10 we find that for most A_t values the relative corrections of our new two-loop corrections are smaller compared to the relative corrections when moving from one- to two-loop order. Note that we cut some of the lines in the middle plot of Fig. 4 (right) as here the relative corrections become artificially large due to comparatively very small widths at the previous loop order. The reduction in the renormalisation scheme dependence when moving from one- to two-loop order is less obvious as can be seen from the lower panel in Fig. 4 (right). The renormalisation scheme dependence becomes artificially large here where the $\overline{\text{DR}}$ result for the partial decay width is very small.

In both scenarios the partial decay widths can become as large as about 1.7 GeV. In P2OS this leads to a branching ratio of about 12% at most, taking into account the dominant decay channels. In BP10 we get a maximum branching ratio of more than 70%.

¹³ Note that, as stated above, the notation for the Higgs states only relates to their dominant component, but still they are mass and not interaction eigenstates.

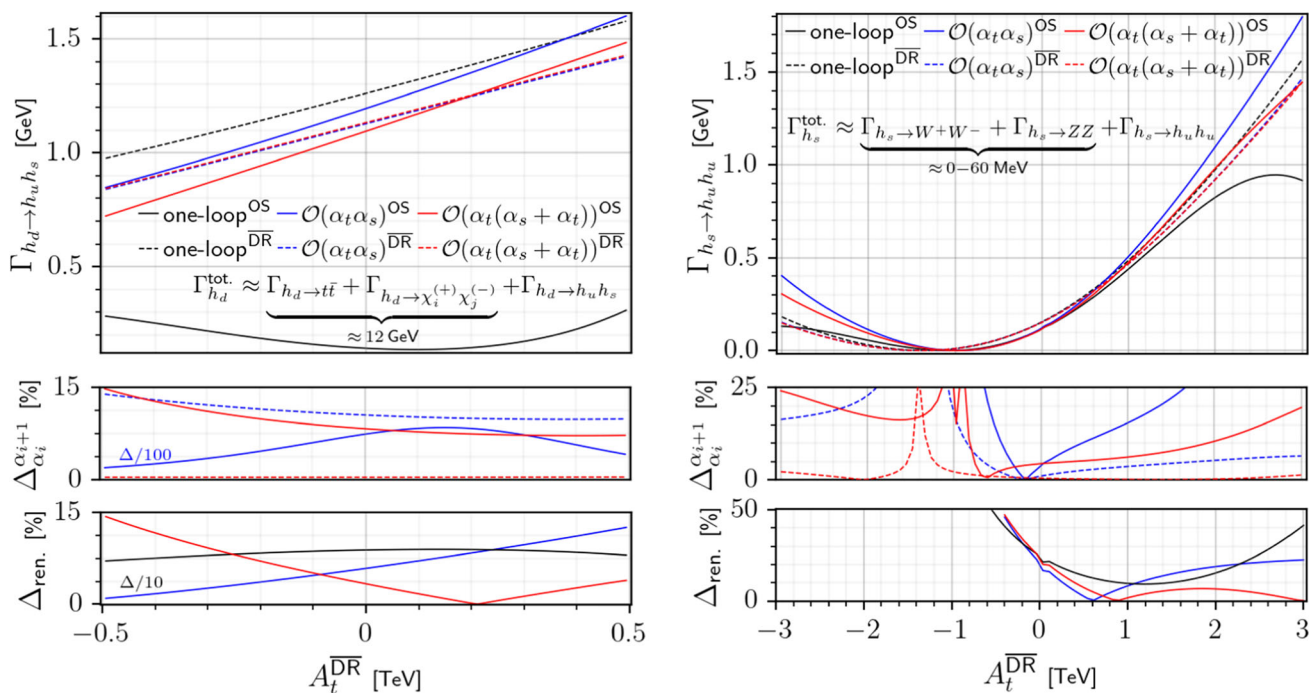


Fig. 4 Upper: Partial decay width of $h_d \rightarrow h_u h_s$ for P2OS (left) and of $h_s \rightarrow h_u h_u$ for BP10 (right) at one-loop order (black), two-loop $\mathcal{O}(\alpha_t \alpha_s)$ (blue) and two-loop $\mathcal{O}(\alpha_t(\alpha_s + \alpha_t))$ (red) in the OS (full) and $\overline{\text{DR}}$ scheme (dashed) as a function of $A_t^{\overline{\text{DR}}}$. In the right plot the dashed blue and red lines nearly lie on top of each other. Middle: The

relative correction defined analogously to Eq. (39), but for the partial decay width. Lower: The relative renormalisation scheme dependence defined analogously to Eq. (40), but for the partial decay width, for all three loop orders

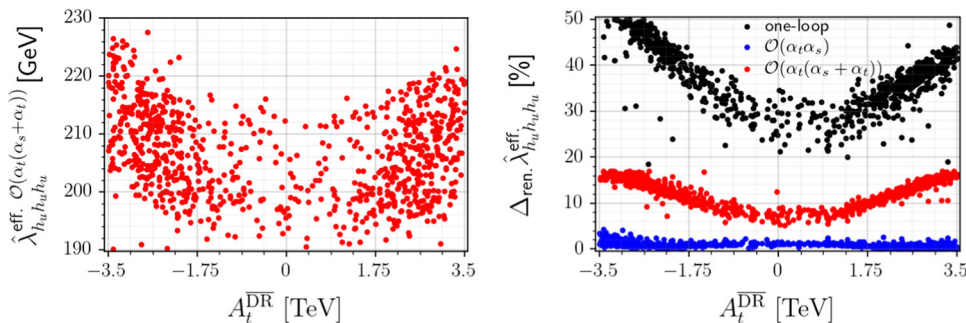


Fig. 5 Left: The effective trilinear self-coupling $\hat{\lambda}_{h_u h_u h_u}^{\text{eff.}}$ of the SM-like h_u -dominated Higgs mass eigenstate as a function of $A_t^{\overline{\text{DR}}}$ at $\mathcal{O}(\alpha_t(\alpha_s + \alpha_t))$ in the OS scheme. Right: The renormalisation scheme

dependence as a function of $A_t^{\overline{\text{DR}}}$ at one-loop order (black), at two-loop $\mathcal{O}(\alpha_t \alpha_s)$ (blue) and at two-loop $\mathcal{O}(\alpha_t(\alpha_s + \alpha_t))$ (red)

Our results show that the higher-order corrections to the decay width have a substantial impact in particular when moving from one-loop to two-loop order. Furthermore, also at the two-loop level the inclusion of the $\mathcal{O}(\alpha_t^2)$ corrections on top of the available $\mathcal{O}(\alpha_t \alpha_s)$ corrections leads to significant changes in the decay width both for P2OS and BP10. At the phenomenological level, the impact of the changes depends on the relative size of the Higgs-to-Higgs decay widths compared to the other decay widths.¹⁴

6 Scatter plots

After the investigation of two specific benchmark points we aim to get an overall picture of the corrections by investigating scatter plots. These plots contain all parameter scenarios that we obtained from our scan and that comply with the included constraints described above. Note that for the scatter plots in order to save computational time, we took a subsample of the parameter points compatible with all constraints.

¹⁴ The partial widths for the computation of the branching ratios are obtained from the code NMSSMCALC [67]. It includes the dominant

higher-order QCD corrections and in the Higgs-to-Higgs decays the higher-order corrections up to $\mathcal{O}(\alpha_t(\alpha_s + \alpha_t))$.

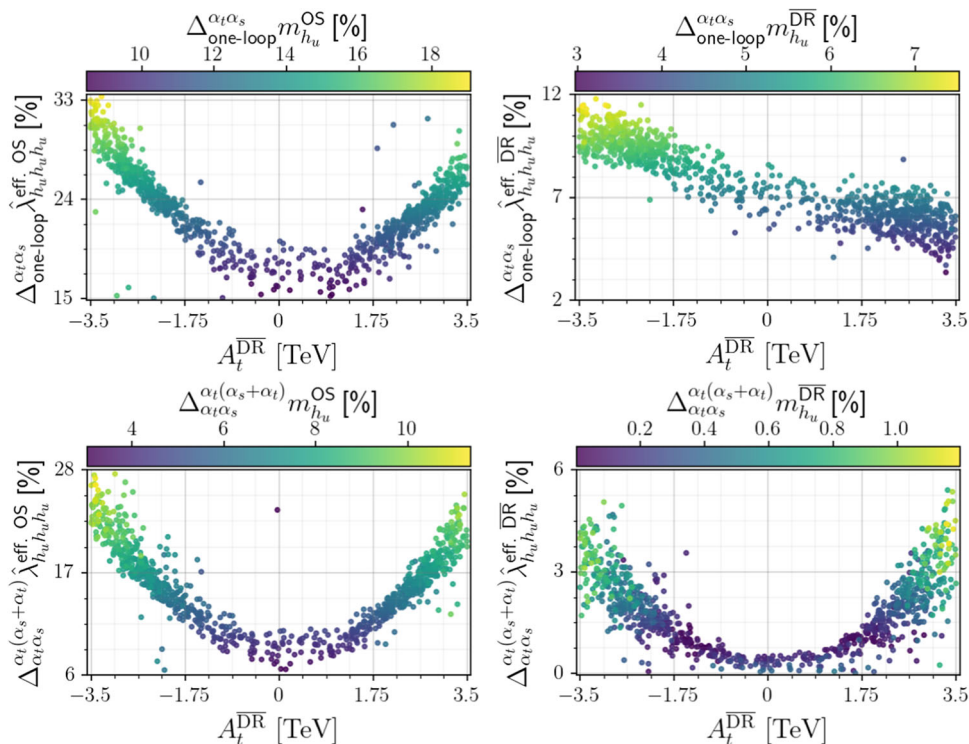


Fig. 6 Relative size of the loop-corrected effective trilinear Higgs self-coupling of the h_u -like Higgs boson $\hat{\lambda}_{h_u h_u h_u}^{\text{eff}}$ w.r.t. the next lower order in the OS (left) and the $\overline{\text{DR}}$ scheme (right) at $\mathcal{O}(\alpha_t \alpha_s)$

(upper) and $\mathcal{O}(\alpha_t(\alpha_s + \alpha_t))$ (lower) as a function of $A_t^{\overline{\text{DR}}}$. The colour bar shows the corresponding values for the h_u -like Higgs mass

It consists of 1k randomly chosen points of the complete sample.

6.1 The trilinear Higgs self-coupling

Figure 5 (left) displays for all generated valid parameter scenarios the effective trilinear Higgs self-coupling $\hat{\lambda}_{h_u h_u h_u}^{\text{eff}}$ of the Higgs mass eigenstate that is dominantly h_u -like, at $\mathcal{O}(\alpha_t(\alpha_s + \alpha_t))$ in the OS renormalisation scheme of the top/stop sector as a function of $A_t \equiv A_t^{\overline{\text{DR}}}$. Note that, depending on the parameter point, the state h_u is not necessarily always the lightest Higgs mass eigenstate. The right plot shows the renormalisation scheme dependence at the one- and considered two-loop orders. We see the same trend as observed for the benchmark points. The scheme dependence at one-loop order is rather large, varying between about 20% and more than 50%. It is considerably reduced upon inclusion of the two-loop $\mathcal{O}(\alpha_t \alpha_s)$ corrections where it ranges between about 1 and 5%. After the additional inclusion of the $\mathcal{O}(\alpha_t^2)$ corrections the scheme dependence increases again to values between 5 and 18% and reflects the necessity to include all corrections at a given loop order in order to make a reliable statement on the scheme dependence. The scheme dependence at two-loop order is well below the one at one-loop level as expected.

Turning to the values of the trilinear Higgs self-coupling $\hat{\lambda}_{h_u h_u h_u}^{\text{eff}}$ we find that it lies between 190 and 228 GeV.¹⁵ For the SM-coupling we have

$$\lambda_{HHH}^{\text{SM}} = \frac{3M_H^2}{v} = 191 \text{ GeV}, \tag{42}$$

for $M_H = 125.09 \text{ GeV}$ and $v = \sqrt{\sqrt{2}G_F} \approx 246.22 \text{ GeV}$. Taking into account the residual theoretical uncertainty at $\mathcal{O}(\alpha_t(\alpha_s + \alpha_t))$ due to missing higher-order corrections, the NMSSM h_u -like trilinear Higgs self-coupling for most of the parameter points complies with the one found in the SM. This means that taking into account the LHC Higgs data results which push the discovered Higgs boson very close to the SM expectation, we find that the NMSSM h_u -like trilinear Higgs self-coupling is also very SM-like once all dominant higher-order corrections are taken into account. This has important implications for the cross section values of Higgs pair production (see our discussion in Sect. 7). Note also that these values for $\hat{\lambda}_{h_u h_u h_u}^{\text{eff}}$ lie well within the present experimental limits on the SM trilinear Higgs self-coupling which are between -0.4 and 6.3 times the SM value as reported by ATLAS [105] and between -1.24 and 6.49 times the SM

¹⁵ Taking into account the whole sample and not only the subsample, there are also a few parameter points that lie outside this range, as e.g. P2OS.

value as found by CMS [106] (both assuming a SM-like top-Yukawa coupling).

6.2 Correlation between trilinear Higgs self-coupling and mass

Figure 6 puts the relative corrections to the effective trilinear Higgs self-coupling of the SM-like h_u -dominated Higgs boson in relation to the relative corrections of its mass value. The scatter plots of the valid parameter scenarios displayed in Fig. 6 (upper) show that the relative impact of the inclusion of the $\mathcal{O}(\alpha_t\alpha_s)$ corrections on top of the one-loop corrections is of about 15–35% in the OS and of roughly 3–12% in the $\overline{\text{DR}}$ scheme for the trilinear Higgs self-coupling. As for the masses, we find here 8–19% in the OS and 3–8% in the $\overline{\text{DR}}$ scheme. Both corrections are correlated, larger corrections in the trilinear Higgs self-coupling correspond to larger corrections for the Higgs mass. As can be inferred from Fig. 6 (lower), the relative size of the additional $\mathcal{O}(\alpha_t^2)$ corrections amounts to about 5–27% in the OS scheme and roughly 1–6% in the $\overline{\text{DR}}$ scheme for the trilinear Higgs self-coupling which compares to 3–11% in the OS scheme and 0.1–1.1% in the $\overline{\text{DR}}$ scheme for the masses. The mass corrections are in general smaller than the corrections to the trilinear Higgs self-couplings, and the corrections in the OS scheme are generally larger than in the $\overline{\text{DR}}$ scheme which partly resums higher-order corrections.

Overall we find for our parameter points compatible with the applied constraints that the effective trilinear Higgs self-coupling values at $\mathcal{O}(\alpha_t(\alpha_s + \alpha_t))$ are in general smaller in the $\overline{\text{DR}}$ scheme compared to the OS scheme, as is the case for the mass values. For both schemes we see that the coupling values increase with increasing mass values. This behavior reflects what we expect from the SM relation Eq. (42), and as stated above, within the residual theoretical uncertainty the trilinear coupling values also comply with the SM result.

7 Higgs pair production

In this section we want to analyse what we can learn from our higher-order results to the trilinear Higgs self-coupling about the impact of the electroweak corrections on Higgs pair production. Higgs pair production gives access to the trilinear Higgs self-coupling and the measurement of the Higgs self-interactions provides the ultimate test [1–4] of the Higgs mechanism for the generation of particle masses. At the LHC the dominant Higgs pair production process is given by gluon fusion into Higgs pairs [1, 107, 108]. The loop-induced process is mediated by top-quark loops and by bottom-quark loops, the latter contributing at the percent level. Higher-order QCD corrections are important, increasing the cross section by roughly a factor two at next-to-leading order

(NLO). A lot of effort is put in providing increasingly precise predictions. The first NLO results were presented in the large top-quark mass limit more than two-decades ago [109]. Full NLO QCD corrections including the top-quark mass dependence were finally made available in [110–113]. The next-to-next-to-leading order (NNLO) QCD corrections in the large m_t limit were provided by [114], and the next-to-next-to-leading logarithmic corrections in this limit by [115, 116]. Recently, the corrections due to the resummation of soft-gluon emission were provided up to next-to-next-to-next-to-leading logarithmic accuracy in [117]. The NNLO $\text{FT}_{\text{approx}}$ ¹⁶ result was presented in [118]. A combination of the usual renormalisation and factorization scale uncertainties with the uncertainties originating from the scheme and scale choice of the virtual top mass was given in [119]. In the NMSSM we have additional diagrams involving top and bottom squarks as well as the s -channel exchange of non-SM-like Higgs bosons, cf. Fig. 7. In [44, 102] we computed the NLO QCD corrections in the heavy-top limit.

So far the complete electroweak (EW) corrections for gluon fusion into Higgs pairs are not yet available. While in the SM we can expect them to be of the order of a few percent by looking at the EW corrections to single Higgs production [120–124] this might not be the case in beyond-the-SM models where couplings can be enhanced compared to the SM or where light Higgs bosons could run in the loops. The computation of the EW corrections to Higgs pair production through gluon fusion is a major task and technical challenge, which requires the computation of massive two-loop integrals with several different mass scales. First steps have been taken recently within the SM. In [125] the top-Yukawa induced part of the EW corrections and their relation to the effective trilinear Higgs coupling have been provided and discussed. The subset of two-loop diagrams where the Higgs boson is exchanged between the virtual top quark lines has been calculated in the high-energy limit in [126].

In this work we use our effective loop-corrected Higgs self-couplings that make up part of the EW corrections to get some insights on their importance. For this we choose the parameter point BP10 where the di-Higgs cross section is dominated by the resonant production of two SM-like Higgs bosons via an intermediate heavy Higgs boson, as in this case the other diagrams will give a subleading contribution to the total cross section so that the missing EW higher-order corrections might be of less importance. In the triangle diagram involving the resonant heavy Higgs boson in the s -channel we still miss, however, the EW corrections to the top triangle.

¹⁶ At $\text{FT}_{\text{approx}}$, the cross section is computed at next-to-next-to-leading order (NNLO) QCD in the heavy-top limit with full leading order (LO) and next-to-leading order (NLO) mass effects and full mass dependence in the one-loop double real corrections at NNLO QCD.

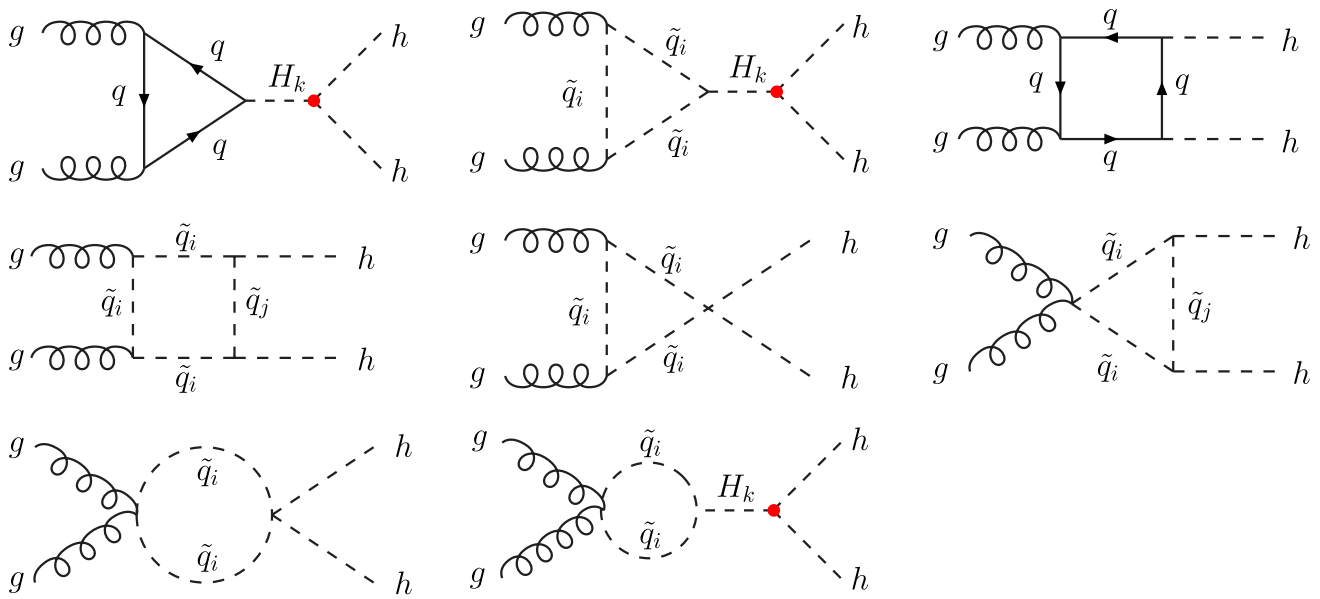


Fig. 7 Generic diagrams contributing to pair production of a SM-like NMSSM Higgs boson h in gluon fusion. The loops involve top and bottom (s)quarks, $q = t, b$, $\tilde{q} = \tilde{t}, \tilde{b}$, $i, j = 1, 2$. The s -channel diagrams

proceed via $H_k = H_1, H_2, H_3$, with one of these being the SM-like h , depending on the parameter choice

For this benchmark point we compute the gluon fusion production cross section for a pair of SM-like Higgs bosons. We choose a c.m. energy of 14 TeV, we use the CT14 pdf set [127] and we set the top quark mass to $m_t = 172.74$ GeV. By using the loop-corrected Higgs masses as inputs and the corresponding higher-order corrected Higgs mixing angles to compute the Yukawa couplings and the trilinear Higgs self-couplings that enter the process through tree-level-like formulae, we take into account the higher-order corrections to the input parameters. By additionally including the loop-corrected trilinear Higgs self-coupling computed in this paper we explicitly include higher-order corrections to the observable, namely the Higgs pair production process, though at an incomplete level as mentioned above.

In Table 4 we compare the di-Higgs cross sections for the case where only corrections to the input parameters are considered (called 'inp' in the following) and the case where we additionally include EW corrections to the process through the loop-corrected trilinear Higgs self-couplings (called 'proc'). For simplicity we focus on the case where we include the full 1-loop corrections both to the masses/mixing angles [75] and to the trilinear Higgs self-couplings [44,45] (named '1L1L') and on the case where we include the 2-loop $\mathcal{O}(\alpha_t(\alpha_s + \alpha_t))$ corrections both to the masses/mixing angles [69] and the trilinear Higgs self-couplings, computed in this paper (named 'at2at2'). We furthermore list in the table the values of the SM-like trilinear Higgs self-coupling, $\lambda_{H_1 H_1 H_1}$, normalized to the SM-value for a Higgs boson mass of same mass value, i.e. $\lambda_{H_1 H_1 H_1}^{\text{SM}} = 3M_{H_1}^2/v$, called $\kappa_{H_1 H_1 H_1}$ in the table. Accordingly, $\kappa_{H_2 H_1 H_1}$ is the $\lambda_{H_2 H_1 H_1}$ coupling normal-

ized to $\lambda_{H_1 H_1 H_1}^{\text{SM}}$. This value is also given in the table as the resonant enhancement of the cross section basically comes from the resonant H_2 production with subsequent decay into $H_1 H_1$. The resonant production from the H_3 decay into $H_1 H_1$ plays only a minor role for this benchmark point. For the 'inp' results we use the trilinear couplings calculated with tree-level-like formulae, for the 'proc' results we use the effective loop-corrected couplings $\hat{\lambda}_{H_1 H_1 H_1}$ and $\hat{\lambda}_{H_2 H_1 H_1}$, respectively. We provide all the loop-corrected values both for OS and $\overline{\text{DR}}$ renormalisation in the top/stop sector. Note that in all renormalisation schemes and at all considered loop levels the Yukawa coupling of the SM-like Higgs H_1 is practically SM-like (it differs by only 1% from the SM-value).

From the cross section values we first of all notice the resonant enhancement compared to the SM Higgs pair production cross section, which at tree-level amounts to 19.72 fb. When we compare the absolute values of the cross section we have to be careful as the changes not only come from the use of different trilinear Higgs self-couplings and renormalisation schemes, but also from the change in the kinematics as the Higgs mass values depend on the loop order and the renormalisation scheme. In the last column of Table 4 we give the relative change of the cross section with respect to the applied renormalisation scheme,

$$\Delta_{\text{ren}}\sigma \equiv \frac{|\sigma^{m_t(\overline{\text{DR}})} - \sigma^{m_t(\text{OS})}|}{\sigma^{m_t(\overline{\text{DR}})}}. \tag{43}$$

We observe that the inclusion of only the parameter corrections does not decrease the renormalisation scheme dependence when moving from one-loop order to two-loop $\mathcal{O}(\alpha_t(\alpha_s + \alpha_t))$, on the contrary. This is not astonishing

Table 4 BP10 : Cross section values for the production of a SM-like Higgs pair $H_1 H_1$ for OS and $\overline{\text{DR}}$ renormalisation in the top/stop sector when using loop-corrected masses and mixing angles ('inp') and additionally loop-corrected effective trilinear Higgs self-couplings ('proc')

'1L1L'	σ^{OS} [fb]	$\sigma^{\overline{\text{DR}}}$ [fb]	$\kappa_{H_1 H_1 H_1}^{\text{OS}}$	$\kappa_{H_1 H_1 H_1}^{\overline{\text{DR}}}$	$\kappa_{H_2 H_1 H_1}^{\text{OS}}$	$\kappa_{H_2 H_1 H_1}^{\overline{\text{DR}}}$	$\Delta_{\text{ren}}\sigma$
'inp'	63.72	62.14	0.54	0.71	-0.25	-0.30	2.5%
'proc'	76.83	61.48	1.01	1.04	-0.30	-0.31	25%
'at2at2'	σ^{OS} [fb]	$\sigma^{\overline{\text{DR}}}$ [fb]	$\kappa_{H_1 H_1 H_1}^{\text{OS}}$	$\kappa_{H_1 H_1 H_1}^{\overline{\text{DR}}}$	$\kappa_{H_2 H_1 H_1}^{\text{OS}}$	$\kappa_{H_2 H_1 H_1}^{\overline{\text{DR}}}$	$\Delta_{\text{ren}}\sigma$
'inp'	68.98	61.25	0.61	0.65	-0.27	-0.28	12.6%
'proc'	71.69	62.57	1.03	1.02	-0.30	-0.31	14.6%

at 1-loop order and at $\mathcal{O}(\alpha_t(\alpha_s + \alpha_t))$, respectively. The corresponding normalized trilinear Higgs self-couplings are given as well as the relative change of the cross section with the applied renormalisation scheme (see the text for definition)

as the scheme dependence of the input parameters has to be compensated by the scheme dependence of the process-dependent corrections at the same loop order. When these are included we observe a decrease in the renormalisation scheme dependence of the cross section at the same loop order when including higher and higher loop orders as expected in perturbation theory. Still the renormalisation scheme dependence with 14.6% at $\mathcal{O}(\alpha_t(\alpha_s + \alpha_t))$ is significant. This gives a hint that the remaining electroweak corrections that we did not take into account in our approach might be significant. It will hence be important to provide the complete EW corrections to the cross section to be able to reduce the uncertainty in its prediction due to missing higher loop corrections.

8 Conclusions

In this paper we presented the $\mathcal{O}(\alpha_t^2)$ corrections to the trilinear Higgs self-couplings in the context of the CP-violating NMSSM. They are part of our ongoing program of increasing the precision in the predictions of the NMSSM Higgs potential parameters, the masses and the Higgs self-couplings. We find that the corrections to the effective trilinear Higgs self-couplings are in general larger than those to the Higgs boson masses. The relative corrections on top of the already existing two-loop corrections at $\mathcal{O}(\alpha_t \alpha_s)$ are much smaller, however, than when moving from one- to two-loop order and indicate perturbative convergence. The remaining residual theoretical uncertainties due to missing higher-order corrections, estimated from the variation of the renormalisation scheme in the top/stop sector, range at the level of a few per-cent and are also reduced compared to the one-loop results. In general, the results obtained in the $\overline{\text{DR}}$ scheme show a better convergence than in the OS scheme, which is to be expected as they already partly resum higher-order corrections. Within the theoretical uncertainties, the obtained loop-corrected trilinear Higgs self-coupling of the SM-like Higgs boson is in accordance with the result for the SM Higgs boson with same

mass value. For our chosen parameter points, the impact of both the one-loop and the two-loop corrections on the Higgs-to-Higgs decay widths is similar to the ones on the effective Higgs self-couplings. The two approaches only differ in the one-loop calculation where we found that in our scenarios the bulk of the one-loop corrections stems from the $\mathcal{O}(\alpha_t)$ corrections that are well approximated by zero external momentum. We also investigated the effect of the inclusion of our loop-corrected effective Higgs self-couplings in the Higgs pair production process. The estimates of the theoretical uncertainty based on the variation of the renormalisation scheme indicate that the remaining missing electroweak corrections to the process may be significant.

Acknowledgements The authors thank M. Spira for discussions on higher-order corrections to Higgs pair production. M.M. and C.B. acknowledge support by the Deutsche Forschungsgemeinschaft (DFG, German Research Foundation) under grant 396021762 - TRR 257. T.N.D. is funded by the Vietnam National Foundation for Science and Technology Development (NAFOSTED) under grant number 103.01-2020.17. H.R.'s research is funded by the Deutsche Forschungsgemeinschaft (DFG, German Research Foundation)—project no. 442089526. MG acknowledges support by the Deutsche Forschungsgemeinschaft (DFG, German Research Foundation) under Germany's Excellence Strategy – EXC 2121 “Quantum Universe”—390833306 and partially by 491245950.

Data Availability Statement This manuscript has no associated data or the data will not be deposited. [Authors' comment: The work presented in this paper does not use any experimental data which needs to be deposited. The input parameters are given in the paper and all the numerical results are either given in the table or displayed in the figures.]

Open Access This article is licensed under a Creative Commons Attribution 4.0 International License, which permits use, sharing, adaptation, distribution and reproduction in any medium or format, as long as you give appropriate credit to the original author(s) and the source, provide a link to the Creative Commons licence, and indicate if changes were made. The images or other third party material in this article are included in the article's Creative Commons licence, unless indicated otherwise in a credit line to the material. If material is not included in the article's Creative Commons licence and your intended use is not permitted by statutory regulation or exceeds the permitted use, you will need to obtain permission directly from the copy-

right holder. To view a copy of this licence, visit <http://creativecommons.org/licenses/by/4.0/>.
Funded by SCOAP³. SCOAP³ supports the goals of the International Year of Basic Sciences for Sustainable Development.

References

- J. Alison et al., Higgs boson potential at colliders: status and perspectives. *Rev. Phys.* **5**, 100045 (2020). <https://doi.org/10.1016/j.revip.2020.100045>. [arXiv:1910.00012](https://arxiv.org/abs/1910.00012)
- A. Djouadi, W. Kilian, M. Muhlleitner, P.M. Zerwas, Testing Higgs selfcouplings at e^+e^- linear colliders. *Eur. Phys. J. C* **10**, 27 (1999). <https://doi.org/10.1007/s100529900082>. [arXiv:hep-ph/9903229](https://arxiv.org/abs/hep-ph/9903229)
- A. Djouadi, W. Kilian, M. Muhlleitner, P.M. Zerwas, Production of neutral Higgs boson pairs at LHC. *Eur. Phys. J. C* **10**, 45 (1999). <https://doi.org/10.1007/s100529900083>. [arXiv:hep-ph/9904287](https://arxiv.org/abs/hep-ph/9904287)
- M.M. Muhlleitner, Higgs particles in the standard model and supersymmetric theories. Ph.D. thesis, Hamburg U (2000). [arXiv:hep-ph/0008127](https://arxiv.org/abs/hep-ph/0008127)
- Y. Golfand, E. Likhtman, Extension of the algebra of poicare group generators and violation of p onvariance. *JETP Lett.* **13**, 323 (1971)
- D.V. Volkov, V.P. Akulov, Is the neutrino a goldstone particle? *Phys. Lett. B* **46**, 109 (1973). [https://doi.org/10.1016/0370-2693\(73\)90490-5](https://doi.org/10.1016/0370-2693(73)90490-5)
- J. Wess, B. Zumino, Supergauge transformations in four-dimensions. *Nucl. Phys. B* **70**, 39 (1974). [https://doi.org/10.1016/0550-3213\(74\)90355-1](https://doi.org/10.1016/0550-3213(74)90355-1)
- P. Fayet, Supergauge invariant extension of the Higgs mechanism and a model for the electron and its neutrino. *Nucl. Phys. B* **90**, 104 (1975). [https://doi.org/10.1016/0550-3213\(75\)90636-7](https://doi.org/10.1016/0550-3213(75)90636-7)
- P. Fayet, Spontaneously broken supersymmetric theories of weak, electromagnetic and strong interactions. *Phys. Lett. B* **69**, 489 (1977). [https://doi.org/10.1016/0370-2693\(77\)90852-8](https://doi.org/10.1016/0370-2693(77)90852-8)
- P. Fayet, S. Ferrara, Supersymmetry. *Phys. Rep.* **32**, 249 (1977). [https://doi.org/10.1016/0370-1573\(77\)90066-7](https://doi.org/10.1016/0370-1573(77)90066-7)
- H.P. Nilles, M. Srednicki, D. Wyler, Weak interaction breakdown induced by supergravity. *Phys. Lett. B* **120**, 346 (1983). [https://doi.org/10.1016/0370-2693\(83\)90460-4](https://doi.org/10.1016/0370-2693(83)90460-4)
- H.P. Nilles, Supersymmetry. Supergravity and particle physics. *Phys. Rep.* **110**, 1 (1984). [https://doi.org/10.1016/0370-1573\(84\)90008-5](https://doi.org/10.1016/0370-1573(84)90008-5)
- J.M. Frere, D.R.T. Jones, S. Raby, Fermion masses and induction of the weak scale by supergravity. *Nucl. Phys. B* **222**, 11 (1983). [https://doi.org/10.1016/0550-3213\(83\)90606-5](https://doi.org/10.1016/0550-3213(83)90606-5)
- J.P. Derendinger, C.A. Savoy, Quantum effects and $SU(2) \times U(1)$ breaking in supergravity gauge theories. *Nucl. Phys. B* **237**, 307 (1984). [https://doi.org/10.1016/0550-3213\(84\)90162-7](https://doi.org/10.1016/0550-3213(84)90162-7)
- H.E. Haber, G.L. Kane, The search for supersymmetry: probing physics beyond the standard model. *Phys. Rep.* **117**, 75 (1985). [https://doi.org/10.1016/0370-1573\(85\)90051-1](https://doi.org/10.1016/0370-1573(85)90051-1)
- M. Sohnius, Introducing supersymmetry. *Phys. Rep.* **128**, 39 (1985). [https://doi.org/10.1016/0370-1573\(85\)90023-7](https://doi.org/10.1016/0370-1573(85)90023-7)
- J.F. Gunion, H.E. Haber, Higgs bosons in supersymmetric models. 1. *Nucl. Phys. B* **272**, 1 (1986). [https://doi.org/10.1016/0550-3213\(86\)90340-8](https://doi.org/10.1016/0550-3213(86)90340-8) (Erratum: *Nucl.Phys.B* **402**, 567–569 (1993))
- J.F. Gunion, H.E. Haber, Higgs bosons in supersymmetric models. 2. Implications for phenomenology. *Nucl. Phys. B* **278**, 449 (1986). [https://doi.org/10.1016/0550-3213\(86\)90050-7](https://doi.org/10.1016/0550-3213(86)90050-7) (Erratum: *Nucl.Phys.B* **402**, 569–569 (1993))
- J.F. Gunion, H.E. Haber, G.L. Kane, S. Dawson, The Higgs Hunter's Guide. *Front. Phys.* **80**, 1–404 (2000)
- S.P. Martin, A supersymmetry primer. *Adv. Ser. Direct. High Energy Phys.* **18**, 1 (1998). https://doi.org/10.1142/9789812839657_0001. [arXiv:hep-ph/9709356](https://arxiv.org/abs/hep-ph/9709356)
- S. Dawson, The MSSM and why it works, in *Theoretical Advanced Study Institute in Elementary Particle Physics (TASI 97)* (Supergravity and Supercolliders, Supersymmetry, 1997), p. 261–339. [arXiv:hep-ph/9712464](https://arxiv.org/abs/hep-ph/9712464)
- A. Djouadi, The anatomy of electro-weak symmetry breaking. II. The Higgs bosons in the minimal supersymmetric model. *Phys. Rep.* **459**, 1 (2008). <https://doi.org/10.1016/j.physrep.2007.10.005>. [arXiv:hep-ph/0503173](https://arxiv.org/abs/hep-ph/0503173)
- G. Aad et al., Combined measurement of the Higgs boson mass in pp collisions at $\sqrt{s} = 7$ and 8 TeV with the ATLAS and CMS experiments. *Phys. Rev. Lett.* **114**, 191803 (2015). <https://doi.org/10.1103/PhysRevLett.114.191803>. [arXiv:1503.07589](https://arxiv.org/abs/1503.07589)
- R. Barbieri, S. Ferrara, C.A. Savoy, Gauge models with spontaneously broken local supersymmetry. *Phys. Lett. B* **119**, 343 (1982). [https://doi.org/10.1016/0370-2693\(82\)90685-2](https://doi.org/10.1016/0370-2693(82)90685-2)
- M. Dine, W. Fischler, M. Srednicki, A simple solution to the strong CP problem with a harmless axion. *Phys. Lett. B* **104**, 199 (1981). [https://doi.org/10.1016/0370-2693\(81\)90590-6](https://doi.org/10.1016/0370-2693(81)90590-6)
- J.R. Ellis, J. Gunion, H.E. Haber, L. Roszkowski, F. Zwirner, Higgs bosons in a nonminimal supersymmetric model. *Phys. Rev. D* **39**, 844 (1989). <https://doi.org/10.1103/PhysRevD.39.844>
- M. Drees, Supersymmetric models with extended Higgs sector. *Int. J. Mod. Phys. A* **4**, 3635 (1989). <https://doi.org/10.1142/S0217751X89001448>
- U. Ellwanger, M. Rausch de Traubenberg, C.A. Savoy, Particle spectrum in supersymmetric models with a gauge singlet. *Phys. Lett. B* **315**, 331 (1993). [https://doi.org/10.1016/0370-2693\(93\)91621-S](https://doi.org/10.1016/0370-2693(93)91621-S). [arXiv:hep-ph/9307322](https://arxiv.org/abs/hep-ph/9307322)
- U. Ellwanger, M. Rausch de Traubenberg, C.A. Savoy, Higgs phenomenology of the supersymmetric model with a gauge singlet. *Z. Phys. C* **67**, 665 (1995). <https://doi.org/10.1007/BF01553993>. [arXiv:hep-ph/9502206](https://arxiv.org/abs/hep-ph/9502206)
- U. Ellwanger, M. Rausch de Traubenberg, C.A. Savoy, Phenomenology of supersymmetric models with a singlet. *Nucl. Phys. B* **492**, 21 (1997). [https://doi.org/10.1016/S0550-3213\(97\)00128-4](https://doi.org/10.1016/S0550-3213(97)00128-4). [arXiv:hep-ph/9611251](https://arxiv.org/abs/hep-ph/9611251)
- T. Elliott, S.F. King, P.L. White, Unification constraints in the next-to-minimal supersymmetric standard model. *Phys. Lett. B* **351**, 213 (1995). [https://doi.org/10.1016/0370-2693\(95\)00381-T](https://doi.org/10.1016/0370-2693(95)00381-T). [arXiv:hep-ph/9406303](https://arxiv.org/abs/hep-ph/9406303)
- S. King, P. White, Resolving the constrained minimal and next-to-minimal supersymmetric standard models. *Phys. Rev. D* **52**, 4183 (1995). <https://doi.org/10.1103/PhysRevD.52.4183>. [arXiv:hep-ph/9505326](https://arxiv.org/abs/hep-ph/9505326)
- F. Franke, H. Fraas, Neutralinos and Higgs bosons in the next-to-minimal supersymmetric standard model. *Int. J. Mod. Phys. A* **12**, 479 (1997). <https://doi.org/10.1142/S0217751X97000529>. [arXiv:hep-ph/9512366](https://arxiv.org/abs/hep-ph/9512366)
- M. Maniatis, The next-to-minimal supersymmetric extension of the Standard Model reviewed. *Int. J. Mod. Phys. A* **25**, 3505 (2010). <https://doi.org/10.1142/S0217751X10049827>. [arXiv:0906.0777](https://arxiv.org/abs/0906.0777)
- U. Ellwanger, C. Hugonie, A.M. Teixeira, The next-to-minimal supersymmetric standard model. *Phys. Rep.* **496**, 1 (2010). <https://doi.org/10.1016/j.physrep.2010.07.001>. [arXiv:0910.1785](https://arxiv.org/abs/0910.1785)
- P. Slavich et al., Higgs-mass predictions in the MSSM and beyond. *Eur. Phys. J. C* **81**(5), 450 (2021). <https://doi.org/10.1140/epjc/s10052-021-09198-2>. [arXiv:2012.15629](https://arxiv.org/abs/2012.15629)
- E.A.R.R.R. Fazio, High-precision calculations of the Higgs Boson mass. *Particles* **5**(1), 53 (2022). <https://doi.org/10.3390/particles5010006>. [arXiv:2112.15295](https://arxiv.org/abs/2112.15295)
- V.D. Barger, M.S. Berger, A.L. Stange, R.J.N. Phillips, Supersymmetric Higgs boson hadroproduction and decays including

- radiative corrections. Phys. Rev. D **45**, 4128 (1992). <https://doi.org/10.1103/PhysRevD.45.4128>
39. W. Hollik, S. Penaranda, Yukawa coupling quantum corrections to the selfcouplings of the lightest MSSM Higgs boson. Eur. Phys. J. C **23**, 163 (2002). <https://doi.org/10.1007/s100520100862>. arXiv:hep-ph/0108245
 40. A. Dobado, M.J. Herrero, W. Hollik, S. Penaranda, Selfinteractions of the lightest MSSM Higgs boson in the large pseudoscalar mass limit. Phys. Rev. D **66**, 095016 (2002). <https://doi.org/10.1103/PhysRevD.66.095016>. arXiv:hep-ph/0208014
 41. K.E. Williams, G. Weiglein, Precise predictions for $h_a \rightarrow h_b h_c$ decays in the complex MSSM. Phys. Lett. B **660**, 217 (2008). <https://doi.org/10.1016/j.physletb.2007.12.049>. arXiv:0710.5320
 42. K.E. Williams, H. Rzehak, G. Weiglein, Higher order corrections to Higgs boson decays in the MSSM with complex parameters. Eur. Phys. J. C **71**, 1669 (2011). <https://doi.org/10.1140/epjc/s10052-011-1669-3>. arXiv:1103.1335
 43. M. Brucherseifer, R. Gavin, M. Spira, Minimal supersymmetric Higgs boson self-couplings: two-loop $O(\alpha_t \alpha_s)$ corrections. Phys. Rev. D **90**(11), 117701 (2014). <https://doi.org/10.1103/PhysRevD.90.117701>. arXiv:1309.3140
 44. D.T. Nhung, M. Mühlleitner, J. Streicher, K. Walz, Higher order corrections to the trilinear Higgs self-couplings in the real NMSSM. JHEP **1311**, 181 (2013). [https://doi.org/10.1007/JHEP11\(2013\)181](https://doi.org/10.1007/JHEP11(2013)181). arXiv:1306.3926
 45. M. Mühlleitner, D.T. Nhung, H. Ziesche, The order $O(\alpha_t \alpha_s)$ corrections to the trilinear Higgs self-couplings in the complex NMSSM. JHEP **12**, 034 (2015). [https://doi.org/10.1007/JHEP12\(2015\)034](https://doi.org/10.1007/JHEP12(2015)034). arXiv:1506.03321
 46. J. Baglio, T.N. Dao, M. Mühlleitner, One-loop corrections to the two-body decays of the neutral Higgs bosons in the complex NMSSM. Eur. Phys. J. C **80**(10), 960 (2020). <https://doi.org/10.1140/epjc/s10052-020-08520-8>. arXiv:1907.12060
 47. S. Kanemura, S. Kiyoura, Y. Okada, E. Senaha, C.P. Yuan, New physics effect on the Higgs selfcoupling. Phys. Lett. B **558**, 157 (2003). [https://doi.org/10.1016/S0370-2693\(03\)00268-5](https://doi.org/10.1016/S0370-2693(03)00268-5). arXiv:hep-ph/0211308
 48. S. Kanemura, Y. Okada, E. Senaha, C.P. Yuan, Higgs coupling constants as a probe of new physics. Phys. Rev. D **70**, 115002 (2004). <https://doi.org/10.1103/PhysRevD.70.115002>. arXiv:hep-ph/0408364
 49. S. Kanemura, M. Kikuchi, K. Yagyu, Fingerprinting the extended Higgs sector using one-loop corrected Higgs boson couplings and future precision measurements. Nucl. Phys. B **896**, 80 (2015). <https://doi.org/10.1016/j.nuclphysb.2015.04.015>. arXiv:1502.07716
 50. S. Kanemura, M. Kikuchi, K. Sakurai, K. Yagyu, Gauge invariant one-loop corrections to Higgs boson couplings in non-minimal Higgs models. Phys. Rev. D **96**(3), 035014 (2017). <https://doi.org/10.1103/PhysRevD.96.035014>. arXiv:1705.05399
 51. P. Basler, M. Mühlleitner, J. Wittbrodt, The CP-violating 2HDM in light of a strong first order electroweak phase transition and implications for Higgs pair production. JHEP **03**, 061 (2018). [https://doi.org/10.1007/JHEP03\(2018\)061](https://doi.org/10.1007/JHEP03(2018)061). arXiv:1711.04097
 52. P. Basler, M. Mühlleitner, J. Müller, Electroweak phase transition in non-minimal Higgs sectors. JHEP **05**, 016 (2020). [https://doi.org/10.1007/JHEP05\(2020\)016](https://doi.org/10.1007/JHEP05(2020)016). arXiv:1912.10477
 53. E. Senaha, Radiative corrections to triple Higgs coupling and electroweak phase transition: beyond one-loop analysis. Phys. Rev. D **100**(5), 055034 (2019). <https://doi.org/10.1103/PhysRevD.100.055034>. arXiv:1811.00336
 54. J. Braathen, S. Kanemura, On two-loop corrections to the Higgs trilinear coupling in models with extended scalar sectors. Phys. Lett. B **796**, 38 (2019). <https://doi.org/10.1016/j.physletb.2019.07.021>. arXiv:1903.05417
 55. J. Braathen, S. Kanemura, Leading two-loop corrections to the Higgs boson self-couplings in models with extended scalar sectors. Eur. Phys. J. C **80**(3), 227 (2020). <https://doi.org/10.1140/epjc/s10052-020-7723-2>. arXiv:1911.11507
 56. H. Bahl, J. Braathen, G. Weiglein, New constraints on extended Higgs sectors from the trilinear Higgs coupling. arXiv:2202.03453
 57. M. Krause, R. Lorenz, M. Mühlleitner, R. Santos, H. Ziesche, Gauge-independent renormalization of the 2-Higgs-doublet model. JHEP **09**, 143 (2016). [https://doi.org/10.1007/JHEP09\(2016\)143](https://doi.org/10.1007/JHEP09(2016)143). arXiv:1605.04853
 58. F. Bojarski, G. Chalons, D. Lopez-Val, T. Robens, Heavy to light Higgs boson decays at NLO in the singlet extension of the Standard Model. JHEP **02**, 147 (2016). [https://doi.org/10.1007/JHEP02\(2016\)147](https://doi.org/10.1007/JHEP02(2016)147). arXiv:1511.08120
 59. M. Krause, D. Lopez-Val, M. Mühlleitner, R. Santos, Gauge-independent renormalization of the N2HDM. JHEP **12**, 077 (2017). [https://doi.org/10.1007/JHEP12\(2017\)077](https://doi.org/10.1007/JHEP12(2017)077). arXiv:1708.01578
 60. M. Krause, M. Mühlleitner, M. Spira, 2HDECAY: a program for the calculation of electroweak one-loop corrections to Higgs decays in the two-Higgs-doublet model including state-of-the-art QCD corrections. Comput. Phys. Commun. **246**, 106852 (2020). <https://doi.org/10.1016/j.cpc.2019.08.003>. arXiv:1810.00768
 61. A. Denner, S. Dittmaier, J.N. Lang, Renormalization of mixing angles. JHEP **11**, 104 (2018). [https://doi.org/10.1007/JHEP11\(2018\)104](https://doi.org/10.1007/JHEP11(2018)104). arXiv:1808.03466
 62. M. Krause, M. Mühlleitner, ewN2HDECAY: a program for the calculation of electroweak one-loop corrections to Higgs decays in the next-to-minimal two-Higgs-doublet model including state-of-the-Art QCD corrections. Comput. Phys. Commun. **247**, 106924 (2020). <https://doi.org/10.1016/j.cpc.2019.106924>. arXiv:1904.02103
 63. M. Krause, M. Mühlleitner, Impact of electroweak corrections on neutral Higgs boson decays in extended Higgs sectors. JHEP **04**, 083 (2020). [https://doi.org/10.1007/JHEP04\(2020\)083](https://doi.org/10.1007/JHEP04(2020)083). arXiv:1912.03948
 64. D. Azevedo, P. Gabriel, M. Mühlleitner, K. Sakurai, R. Santos, One-loop corrections to the Higgs boson invisible decay in the dark doublet phase of the N2HDM. JHEP **10**, 044 (2021). [https://doi.org/10.1007/JHEP10\(2021\)044](https://doi.org/10.1007/JHEP10(2021)044). arXiv:2104.03184
 65. F. Egle, M. Mühlleitner, R. Santos, J.A. Viana, One-loop corrections to the Higgs boson invisible decay in a complex singlet extension of the SM. arXiv:2202.04035
 66. M.D. Goodsell, S. Liebler, F. Staub, Generic calculation of two-body partial decay widths at the full one-loop level. Eur. Phys. J. C **77**(11), 758 (2017). <https://doi.org/10.1140/epjc/s10052-017-5259-x>. arXiv:1703.09237
 67. J. Baglio, R. Gröber, M. Mühlleitner, D.T. Nhung, H. Rzehak, M. Spira, J. Streicher, K. Walz, NMSSMCALC: a program package for the calculation of loop-corrected Higgs boson masses and decay widths in the (Complex) NMSSM. Comput. Phys. Commun. **185**(12), 3372 (2014). <https://doi.org/10.1016/j.cpc.2014.08.005>. arXiv:1312.4788
 68. S.F. King, M. Mühlleitner, R. Nevzorov, K. Walz, Exploring the CP-violating NMSSM: EDM constraints and phenomenology. Nucl. Phys. B **901**, 526 (2015). <https://doi.org/10.1016/j.nuclphysb.2015.11.003>. arXiv:1508.03255
 69. T. Dao, R. Gröber, M. Krause, M. Mühlleitner, H. Rzehak, Two-loop $O(\alpha_t^2)$ corrections to the neutral Higgs boson masses in the CP-violating NMSSM. JHEP **08**, 114 (2019). [https://doi.org/10.1007/JHEP08\(2019\)114](https://doi.org/10.1007/JHEP08(2019)114)
 70. M. Mühlleitner, D.T. Nhung, H. Rzehak, K. Walz, Two-loop contributions of the order $mathcal{O}(\alpha_t \alpha_s)$ to the masses of the Higgs bosons in the CP-violating NMSSM. JHEP **05**, 128 (2015). [https://doi.org/10.1007/JHEP05\(2015\)128](https://doi.org/10.1007/JHEP05(2015)128). arXiv:1412.0918

71. T.N. Dao, M. Gabelmann, M. Mühlleitner, H. Rzehak, Two-loop $\mathcal{O}(\alpha_t + \alpha_\lambda + \alpha_\kappa)^2$ corrections to the Higgs boson masses in the CP-violating NMSSM. JHEP **09**, 193 (2021). [https://doi.org/10.1007/JHEP09\(2021\)193](https://doi.org/10.1007/JHEP09(2021)193). arXiv:2106.06990
72. P.Z. Skands et al., SUSY Les Houches accord: Interfacing SUSY spectrum calculators, decay packages, and event generators. JHEP **07**, 036 (2004). <https://doi.org/10.1088/1126-6708/2004/07/036>
73. B.C. Allanach et al., SUSY Les Houches Accord 2. Comput. Phys. Commun. **180**, 8 (2009). <https://doi.org/10.1016/j.cpc.2008.08.004>. arXiv:0801.0045
74. K. Ender, T. Graf, M. Mühlleitner, H. Rzehak, Analysis of the NMSSM Higgs boson masses at one-loop level. Phys. Rev. D **85**, 075024 (2012). <https://doi.org/10.1103/PhysRevD.85.075024>
75. T. Graf, R. Grober, M. Mühlleitner, H. Rzehak, K. Walz, Higgs Boson masses in the complex NMSSM at one-loop level. JHEP **10**, 122 (2012). [https://doi.org/10.1007/JHEP10\(2012\)122](https://doi.org/10.1007/JHEP10(2012)122)
76. A.I. Davydchev, J. Tausk, Two loop selfenergy diagrams with different masses and the momentum expansion. Nucl. Phys. B **397**, 123 (1993). [https://doi.org/10.1016/0550-3213\(93\)90338-P](https://doi.org/10.1016/0550-3213(93)90338-P)
77. C. Ford, I. Jack, D. Jones, The Standard model effective potential at two loops. Nucl. Phys. B **387**, 373 (1992). [https://doi.org/10.1016/0550-3213\(92\)90165-8](https://doi.org/10.1016/0550-3213(92)90165-8) (Erratum: Nucl. Phys. B **504**, 551–552 (1997))
78. R. Scharf, J. Tausk, Scalar two loop integrals for gauge boson selfenergy diagrams with a massless fermion loop. Nucl. Phys. B **412**, 523 (1994). [https://doi.org/10.1016/0550-3213\(94\)90391-3](https://doi.org/10.1016/0550-3213(94)90391-3)
79. G. Weiglein, R. Scharf, M. Bohm, Reduction of general two loop selfenergies to standard scalar integrals. Nucl. Phys. B **416**, 606 (1994). [https://doi.org/10.1016/0550-3213\(94\)90325-5](https://doi.org/10.1016/0550-3213(94)90325-5). arXiv:hep-ph/9310358
80. F.A. Berends, J.B. Tausk, On the numerical evaluation of scalar two loop selfenergy diagrams. Nucl. Phys. B **421**, 456 (1994). [https://doi.org/10.1016/0550-3213\(94\)90336-0](https://doi.org/10.1016/0550-3213(94)90336-0)
81. S.P. Martin, Two loop effective potential for a general renormalizable theory and softly broken supersymmetry. Phys. Rev. D **65**, 116003 (2002). <https://doi.org/10.1103/PhysRevD.65.116003>. arXiv:hep-ph/0111209
82. S.P. Martin, D.G. Robertson, TSIL: a program for the calculation of two-loop self-energy integrals. Comput. Phys. Commun. **174**, 133 (2006). <https://doi.org/10.1016/j.cpc.2005.08.005>
83. F. Staub, SARAH. arXiv:0806.0538
84. F. Staub, Automatic calculation of supersymmetric renormalization group equations and self energies. Comput. Phys. Commun. **182**, 808 (2011). <https://doi.org/10.1016/j.cpc.2010.11.030>. arXiv:1002.0840
85. F. Staub, SARAH 3.2: Dirac Gauginos, UFO output, and more. Comput. Phys. Commun. **184**, 1792 (2013). <https://doi.org/10.1016/j.cpc.2013.02.019>. arXiv:1207.0906
86. F. Staub, SARAH 4: a tool for (not only SUSY) model builders. Comput. Phys. Commun. **185**, 1773 (2014). <https://doi.org/10.1016/j.cpc.2014.02.018>. arXiv:1309.7223
87. M.D. Goodsell, K. Nickel, F. Staub, Two-loop Higgs mass calculations in supersymmetric models beyond the MSSM with SARAH and SPheno. Eur. Phys. J. C **75**(1), 32 (2015). <https://doi.org/10.1140/epjc/s10052-014-3247-y>. arXiv:1411.0675
88. M.D. Goodsell, K. Nickel, F. Staub, Two-loop corrections to the Higgs masses in the NMSSM. Phys. Rev. D **91**, 035021 (2015). <https://doi.org/10.1103/PhysRevD.91.035021>. arXiv:1411.4665
89. J. Kublbeck, M. Bohm, A. Denner, Feyn arts: computer algebraic generation of Feynman graphs and amplitudes. Comput. Phys. Commun. **60**, 165 (1990). [https://doi.org/10.1016/0010-4655\(90\)90001-H](https://doi.org/10.1016/0010-4655(90)90001-H)
90. T. Hahn, Generating Feynman diagrams and amplitudes with FeynArts 3. Comput. Phys. Commun. **140**, 418 (2001). [https://doi.org/10.1016/S0010-4655\(01\)00290-9](https://doi.org/10.1016/S0010-4655(01)00290-9). arXiv:hep-ph/0012260
91. R. Mertig, M. Bohm, A. Denner, FEYN CALC: computer algebraic calculation of Feynman amplitudes. Comput. Phys. Commun. **64**, 345 (1991). [https://doi.org/10.1016/0010-4655\(91\)90130-D](https://doi.org/10.1016/0010-4655(91)90130-D)
92. V. Shtabovenko, R. Mertig, F. Orellana, New developments in FeynCalc 9.0. Comput. Phys. Commun. **207**, 432 (2016). <https://doi.org/10.1016/j.cpc.2016.06.008>. arXiv:1601.01167
93. R. Mertig, R. Scharf, TARCER: A Mathematica program for the reduction of two loop propagator integrals. Comput. Phys. Commun. **111**, 265 (1998). [https://doi.org/10.1016/S0010-4655\(98\)00042-3](https://doi.org/10.1016/S0010-4655(98)00042-3). arXiv:hep-ph/9801383
94. P. Bechtle, O. Brein, S. Heinemeyer, G. Weiglein, K.E. Williams, HiggsBounds: confronting arbitrary Higgs sectors with exclusion bounds from LEP and the tevatron. Comput. Phys. Commun. **181**, 138 (2010). <https://doi.org/10.1016/j.cpc.2009.09.003>. arXiv:0811.4169
95. P. Bechtle, O. Brein, S. Heinemeyer, G. Weiglein, K.E. Williams, HiggsBounds 2.0.0: confronting neutral and charged Higgs sector predictions with exclusion bounds from LEP and the tevatron. Comput. Phys. Commun. **182**, 2605 (2011). <https://doi.org/10.1016/j.cpc.2011.07.015>. arXiv:1102.1898
96. P. Bechtle, O. Brein, S. Heinemeyer, O. Stål, T. Stefaniak, G. Weiglein, K.E. Williams, HiggsBounds – 4: improved tests of extended Higgs sectors against exclusion bounds from LEP, the tevatron and the LHC. Eur. Phys. J. C **74**(3), 2693 (2014). <https://doi.org/10.1140/epjc/s10052-013-2693-2>
97. P. Bechtle, S. Heinemeyer, O. Stål, T. Stefaniak, G. Weiglein, HiggsSignals: confronting arbitrary Higgs sectors with measurements at the tevatron and the LHC. Eur. Phys. J. C **74**(2), 2711 (2014). <https://doi.org/10.1140/epjc/s10052-013-2711-4>. arXiv:1305.1933
98. M. Tanabashi et al., Review of particle physics. Phys. Rev. D **98**, 030001 (2018). <https://doi.org/10.1103/PhysRevD.98.030001>
99. A. Denner, S. Dittmaier, M. Grazzini, R.V. Harlander, R.S. Thorne, M. Spira, M. Steinhauser, Standard Model input parameters for Higgs physics. LHCHSWG-INT-2015-006
100. ATLAS, SUSY Summary Plots (June 2021). ATL-PHYS-PUB-2021-019
https://twiki.cern.ch/twiki/bin/view/CMSPublic/PhysicsResultsSUS#Run_2_Summary_Plots_13_TeV
101. CMS.
102. H. Abouabid, A. Arhrib, D. Azevedo, J.E. Falaki, P.M. Ferreira, M. Mühlleitner, R. Santos, Benchmarking Di-Higgs production in various extended Higgs sector models. arXiv:2112.12515
103. S. Inoue, M.J. Ramsey-Musolf, Y. Zhang, CP-violating phenomenology of flavor conserving two Higgs doublet models. Phys. Rev. D **89**(11), 115023 (2014). <https://doi.org/10.1103/PhysRevD.89.115023>. arXiv:1403.4257
104. J. Baron et al., Order of magnitude smaller limit on the electric dipole moment of the electron. Science **343**, 269 (2014). <https://doi.org/10.1126/science.1248213>. arXiv:1310.7534
105. A. Collaboration, Constraining the Higgs boson self-coupling from single- and double-Higgs production with the ATLAS detector using pp collisions at $\sqrt{s}=13$ TeV. ATLAS-CONF-2022-50
106. A portrait of the Higgs boson by the CMS experiment ten years after the discovery. Nature **607**(7917), 60 (2022). <https://doi.org/10.1038/s41586-022-04892-x>. arXiv:2207.00043
107. D. de Florian, et al., Handbook of LHC Higgs Cross Sections: 4. Deciphering the nature of the higgs sector. CERN Yellow Reports: Monographs **2/2017**. <https://doi.org/10.23731/CYRM-2017-002>. arXiv:1610.07922
108. J. Baglio, A. Djouadi, R. Gröber, M.M. Mühlleitner, J. Quevillon, M. Spira, The measurement of the Higgs self-coupling at the LHC: theoretical status. JHEP **04**, 151 (2013). [https://doi.org/10.1007/JHEP04\(2013\)151](https://doi.org/10.1007/JHEP04(2013)151). arXiv:1212.5581
109. S. Dawson, S. Dittmaier, M. Spira, Neutral Higgs boson pair production at hadron colliders: QCD corrections. Phys. Rev.

- D **58**, 115012 (1998). <https://doi.org/10.1103/PhysRevD.58.115012>. [arXiv:hep-ph/9805244](https://arxiv.org/abs/hep-ph/9805244)
110. S. Borowka, N. Greiner, G. Heinrich, S.P. Jones, M. Kerner, J. Schlenk, U. Schubert, T. Zirke, Higgs Boson pair production in gluon fusion at next-to-leading order with full top-quark mass dependence. *Phys. Rev. Lett.* **117**(1), 012001 (2016). <https://doi.org/10.1103/PhysRevLett.117.079901> (**Erratum: Phys.Rev.Lett.** **117**, 079901 (2016)). [arXiv:1604.06447](https://arxiv.org/abs/1604.06447)
111. S. Borowka, N. Greiner, G. Heinrich, S.P. Jones, M. Kerner, J. Schlenk, T. Zirke, Full top quark mass dependence in Higgs boson pair production at NLO. *JHEP* **10**, 107 (2016). [https://doi.org/10.1007/JHEP10\(2016\)107](https://doi.org/10.1007/JHEP10(2016)107). [arXiv:1608.04798](https://arxiv.org/abs/1608.04798)
112. J. Baglio, F. Campanario, S. Glaus, M. Mühlleitner, M. Spira, J. Streicher, Gluon fusion into Higgs pairs at NLO QCD and the top mass scheme. *Eur. Phys. J. C* **79**(6), 459 (2019). <https://doi.org/10.1140/epjc/s10052-019-6973-3>. [arXiv:1811.05692](https://arxiv.org/abs/1811.05692)
113. J. Baglio, F. Campanario, S. Glaus, M. Mühlleitner, J. Ronca, M. Spira, J. Streicher, Higgs-pair production via gluon fusion at hadron colliders: NLO QCD Corrections. *JHEP* **04**, 181 (2020). [https://doi.org/10.1007/JHEP04\(2020\)181](https://doi.org/10.1007/JHEP04(2020)181). [arXiv:2003.03227](https://arxiv.org/abs/2003.03227)
114. D. de Florian, J. Mazzitelli, Higgs Boson pair production at next-to-next-to-leading order in QCD. *Phys. Rev. Lett.* **111**, 201801 (2013). <https://doi.org/10.1103/PhysRevLett.111.201801>. [arXiv:1309.6594](https://arxiv.org/abs/1309.6594)
115. D.Y. Shao, C.S. Li, H.T. Li, J. Wang, Threshold resummation effects in Higgs boson pair production at the LHC. *JHEP* **07**, 169 (2013). [https://doi.org/10.1007/JHEP07\(2013\)169](https://doi.org/10.1007/JHEP07(2013)169). [arXiv:1301.1245](https://arxiv.org/abs/1301.1245)
116. D. de Florian, J. Mazzitelli, Higgs pair production at next-to-next-to-leading logarithmic accuracy at the LHC. *JHEP* **09**, 053 (2015). [https://doi.org/10.1007/JHEP09\(2015\)053](https://doi.org/10.1007/JHEP09(2015)053). [arXiv:1505.07122](https://arxiv.org/abs/1505.07122)
117. A.H. Ajjath, H.S. Shao, $N^3\text{LO}+N^3\text{LL}$ QCD improved Higgs pair cross sections. [arXiv:2209.03914](https://arxiv.org/abs/2209.03914)
118. M. Grazzini, G. Heinrich, S. Jones, S. Kallweit, M. Kerner, J.M. Lindert, J. Mazzitelli, Higgs boson pair production at NNLO with top quark mass effects. *JHEP* **05**, 059 (2018). [https://doi.org/10.1007/JHEP05\(2018\)059](https://doi.org/10.1007/JHEP05(2018)059). [arXiv:1803.02463](https://arxiv.org/abs/1803.02463)
119. J. Baglio, F. Campanario, S. Glaus, M. Mühlleitner, J. Ronca, M. Spira, $gg \rightarrow HH$: combined uncertainties. *Phys. Rev. D* **103**(5), 056002 (2021). <https://doi.org/10.1103/PhysRevD.103.056002>. [arXiv:2008.11626](https://arxiv.org/abs/2008.11626)
120. A. Djouadi, P. Gambino, Leading electroweak correction to Higgs boson production at proton colliders. *Phys. Rev. Lett.* **73**, 2528 (1994). <https://doi.org/10.1103/PhysRevLett.73.2528>. [arXiv:hep-ph/9406432](https://arxiv.org/abs/hep-ph/9406432)
121. U. Aglietti, R. Bonciani, G. Degrassi, A. Vicini, Two loop light fermion contribution to Higgs production and decays. *Phys. Lett. B* **595**, 432 (2004). <https://doi.org/10.1016/j.physletb.2004.06.063>. [arXiv:hep-ph/0404071](https://arxiv.org/abs/hep-ph/0404071)
122. G. Degrassi, F. Maltoni, Two-loop electroweak corrections to Higgs production at hadron colliders. *Phys. Lett. B* **600**, 255 (2004). <https://doi.org/10.1016/j.physletb.2004.09.008>. [arXiv:hep-ph/0407249](https://arxiv.org/abs/hep-ph/0407249)
123. S. Actis, G. Passarino, C. Sturm, S. Uccirati, NNLO computational techniques: the cases $H \rightarrow \gamma\gamma$ and $H \rightarrow g g$. *Nucl. Phys. B* **811**, 182 (2009). <https://doi.org/10.1016/j.nuclphysb.2008.11.024>. [arXiv:0809.3667](https://arxiv.org/abs/0809.3667)
124. S. Actis, G. Passarino, C. Sturm, S. Uccirati, NLO electroweak corrections to Higgs boson production at hadron colliders. *Phys. Lett. B* **670**, 12 (2008). <https://doi.org/10.1016/j.physletb.2008.10.018>. [arXiv:0809.1301](https://arxiv.org/abs/0809.1301)
125. M. Mühlleitner, J. Schlenk, M. Spira, Top-Yukawa-induced corrections to Higgs pair production. [arXiv:2207.02524](https://arxiv.org/abs/2207.02524)
126. J. Davies, G. Mishima, K. Schönwald, M. Steinhauser, H. Zhang, Higgs boson contribution to the leading two-loop Yukawa corrections to $gg \rightarrow HH$. [arXiv:2207.02587](https://arxiv.org/abs/2207.02587)
127. S. Dulat, T.J. Hou, J. Gao, M. Guzzi, J. Huston, P. Nadolsky, J. Pumplin, C. Schmidt, D. Stump, C.P. Yuan, New parton distribution functions from a global analysis of quantum chromodynamics. *Phys. Rev. D* **93**(3), 033006 (2016). <https://doi.org/10.1103/PhysRevD.93.033006>. [arXiv:1506.07443](https://arxiv.org/abs/1506.07443)